

# Cranial anatomy of a new genus of hyperodapedontine rhynchosaur (Diapsida, Archosauromorpha) from the Upper Triassic of southern Brazil

Felipe Chinaglia Montefeltro<sup>1</sup>, Max Cardoso Langer<sup>1</sup> and Cesar Leandro Schultz<sup>2</sup>

<sup>1</sup> Laboratório de Paleontologia, Departamento de Biologia, Faculdade de Filosofia, Ciências e Letras de Ribeirão Preto, Universidade de São Paulo, Av. Bandeirantes 3900, 14040-901, Ribeirão Preto SP, Brazil  
Email: felipecm@pg.ffclrp.usp.br; mclanger@ffclrp.usp.br

<sup>2</sup> Departamento de Paleontologia e Estratigrafia, Universidade Federal do Rio Grande do Sul, Av. Bento Gonçalves 9500, 91540-000 Porto Alegre RS, Brazil  
Email: cesar.schultz@ufrgs.br

**ABSTRACT:** Detailed description of the cranial anatomy of the rhynchosaur previously known as *Scaphonyx sulcognathus* allows its assignment to a new genus *Teyumbaita*. Two nearly complete skulls and a partial skull have been referred to the taxon, all of which come from the lower part of the Caturrita Formation, Upper Triassic of Rio Grande do Sul, southern Brazil. Cranial autapomorphies of *Teyumbaita sulcognathus* include anterior margin of nasal concave at midline, prefrontal separated from the ascending process of the maxilla, palatal ramus of pterygoid expanded laterally within palatines, dorsal surface of exoccipital markedly depressed, a single tooth lingually displaced from the main medial tooth-bearing area of the maxilla, and a number of other characters (such as skull broader than long; a protruding orbital anterior margin; *anguli oris* extending to anterior ramus of the jugal; bar between the orbit and the lower temporal fenestra wider than 0.4 of the total orbital opening; mandibular depth reaching more than 25% of the total length) support its inclusion in Hyperodapedontinae. *T. sulcognathus* is the only potential Norian rhynchosaur, suggesting that the group survived the end-Carnian extinction event.

**KEY WORDS:** Caturrita Formation, Norian, Rhynchosauria, skull anatomy, *Teyumbaita sulcognathus*

Rhynchosaurs represent a well-supported monophyletic group of basal herbivorous archosauromorphs (Benton 1984a, 1985; Evans 1988; Dilkes 1995, 1998) known from Triassic terrestrial deposits. Early Middle Triassic forms (Rubidge 2005) occur in the *Cynognathus* assemblage subzone B (Karoo Group) of South Africa, but the clade experienced a rapid radiation. Thereafter they reached an almost global distribution by late Triassic times, becoming the most common herbivorous tetrapods in various dry-land areas of the time. The relatively well-known record of rhynchosaurs illustrates a classic case of ‘explosive evolution’ (Romer 1962) that matches the taxonomic and phylogenetic hypotheses proposed for the group. *Mesosuchus browni* consensually occupies the basal-most position, followed by a coeval form, *Howesia browni*, as the sister taxon of later rhynchosaurs, i.e., Rhynchosauridae (Benton 1984a, 1985, 1988, 1990; Evans 1988; Dilkes 1995, 1998; Hone & Benton 2008).

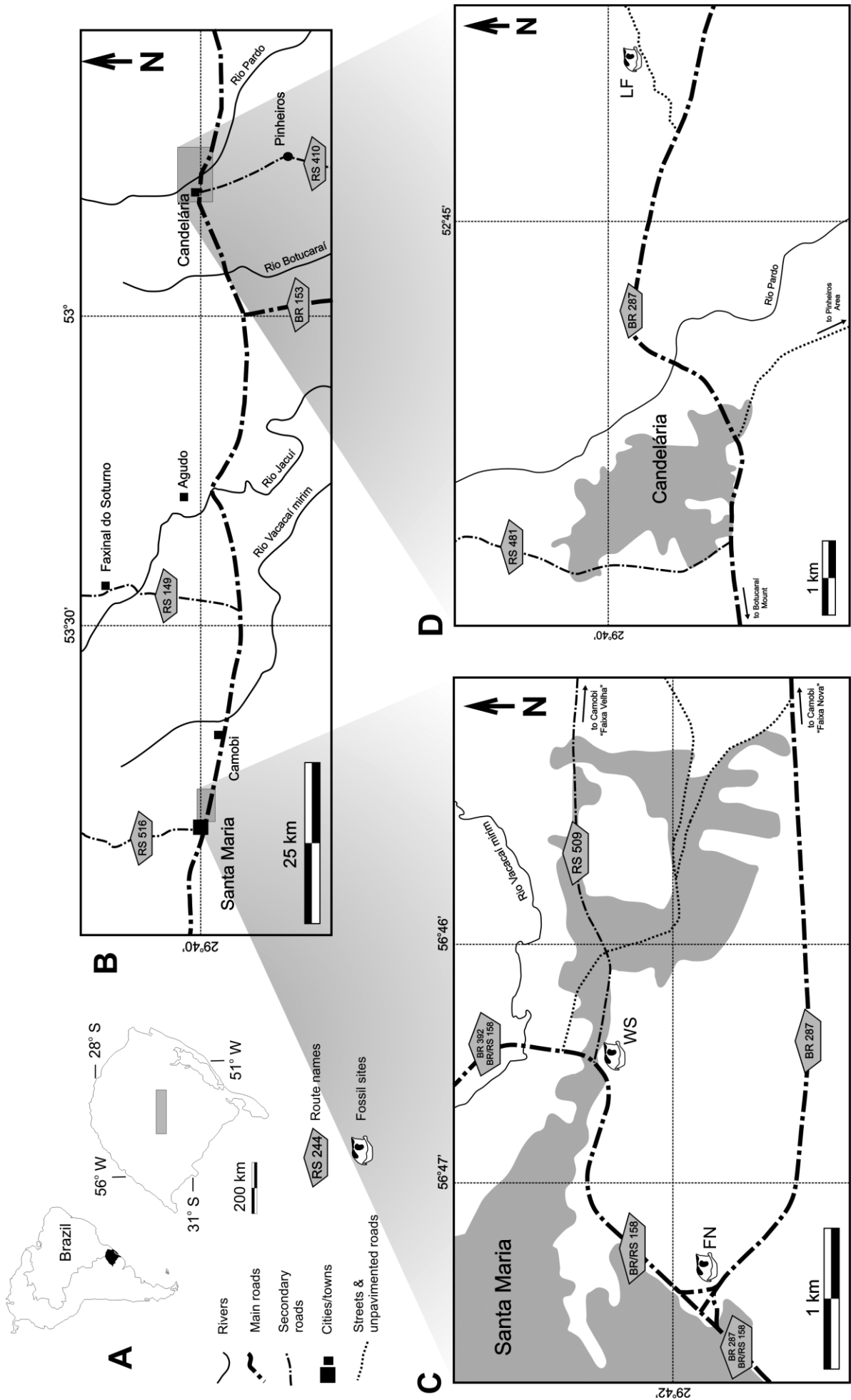
Rhynchosaurids are the typical rhynchosaurs, bearing tusk-like downturned premaxillae and a blade and groove jaw apparatus. Despite the ambiguous relationships of its basal forms (see Langer & Schultz 2000a; Hone & Benton 2008), Late Triassic taxa are recognised as forming the Hyperodapedontinae clade (Chatterjee 1969; Benton 1988, 1990; Dilkes 1995, 1998; Langer & Schultz 2000a; Langer *et al.* 2000a; Hone & Benton 2008). This has been recognised since the 19th

Century (Lydekker 1885, 1888; Huxley 1887), when *Hyperodapedon gordonii* from northern Scotland and *H. huxleyi* from India were grouped separately from the other rhynchosaurid known at the time, *Rhynchosaurus articeps* from the English Midlands.

The description of *Scaphonyx fischeri* (Woodward 1907) from southern Brazil, and later revisions (Huene 1926, 1929, 1939, 1942; Sill 1970) established the genus *Scaphonyx* as the sole South American Late Triassic rhynchosaur genus. Within this paradigm, Azevedo & Schultz (1987) described a new taxon from the lower levels of the Caturrita Formation, Upper Triassic of southern Brazil, as *S. sulcognathus*. Following new discoveries and taxonomic revisions (Langer & Schultz 2000a), the much greater diversity of Upper Triassic South American rhynchosaurs was recognised. In this context the holotype of *Scaphonyx fischeri* (composed of phalanges and vertebral centra) was regarded as undiagnostic of any particular form, and the binomen was considered a *nomen dubium* (Langer & Schultz 2000b). The rhynchosaurs previously ascribed to *Scaphonyx* were then referred to both *Hyperodapedon mariensis* and *H. sanjuanensis* (Langer & Schultz 2000a, b).

Despite its full acceptance as a unique genus (Langer & Schultz 2000a, b; Langer *et al.* 2000a, b, 2007; Hone & Benton 2008), recent work failed to erect a new genus for ‘*Scaphonyx sulcognathus*’. This was probably awaiting a full description of





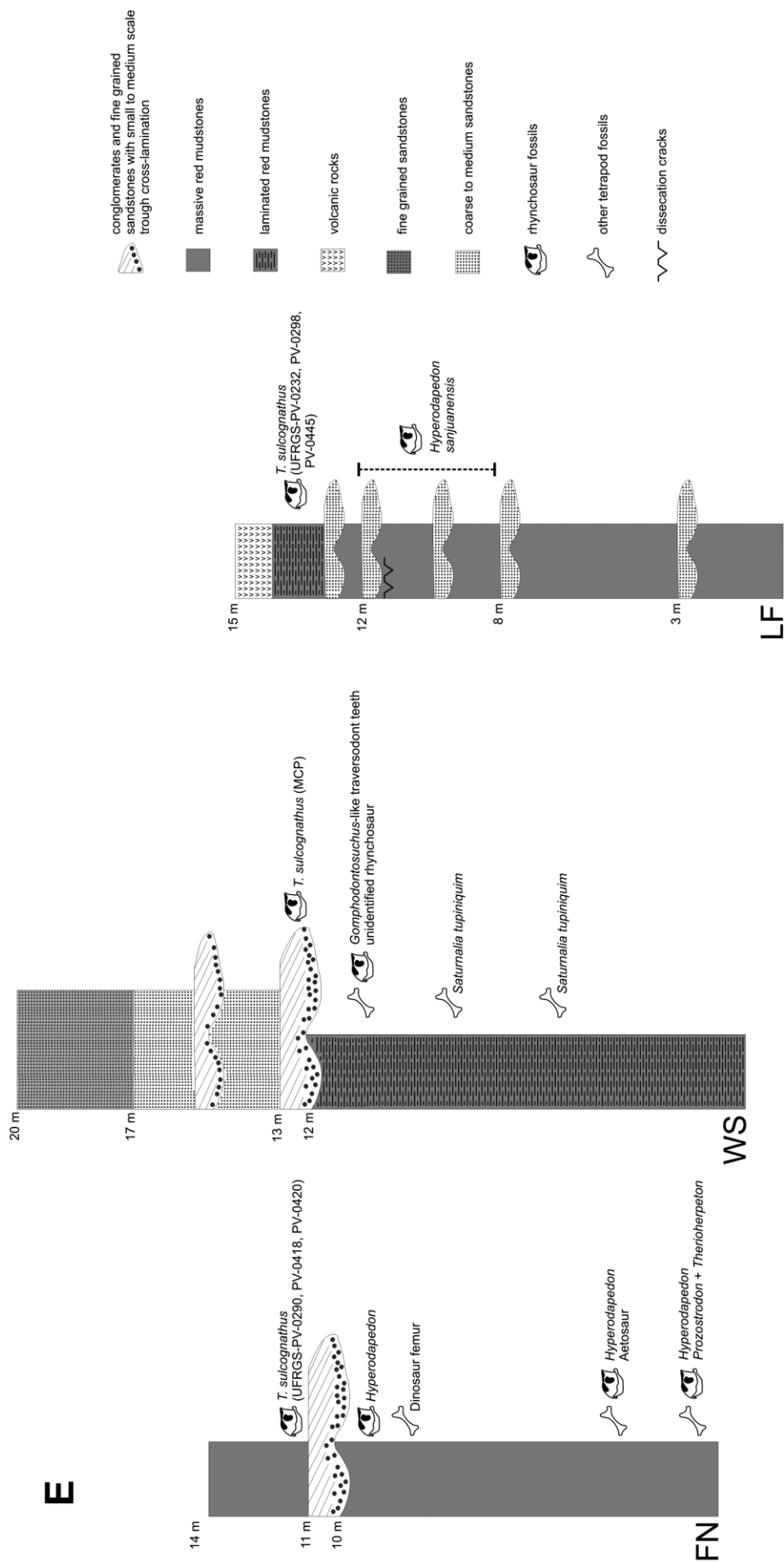


**Figure 1** Localities that have yielded specimens of *Teyumbaita sulcognathus*: (A) Location map of Rio Grande do Sul within South America; (B) Area between Santa Maria and Candelária, highlighted in Figure 1A; (C) Eastern outskirts of Santa Maria, showing the sites of Faixa Nova and Waldsanga; (D) Candelária area, showing the type-locality (Linha Facão) of *T. sulcognathus*; (E) Stratigraphic sections of Faixa Nova (FN), Waldsanga (WS) and Linha Facão (LF).

the referred specimens, which is provided in the present paper. Published data on '*Scaphonyx*' *sulcognathus* is limited. Anatomical information is restricted to unpublished theses (Azevedo 1982; Schultz 1986, 1991; Langer 1996) or codifications and sparse considerations in phylogenetic studies (Langer & Schultz 2000a, b; Langer *et al.* 2000a; Hone & Benton 2008). The aim of the present paper is to revise and describe the cranial remains of this endemic Brazilian Upper Triassic rhynchosaur, establishing a new genus.

All specimens related to the new genus come from sites within the central region of Rio Grande do Sul State, Brazil (Fig. 1). The holotype, UFRGS PV-0298T and PV-0445T come from Linha Facão (29°40'12"S; 52°43'30"W) in the area of Candelária. MCP-683 comes from Huene's (1942) Waldsanga site (29°41'51.8"S; 53°46'27"W) and the other three specimens from Faixa Nova (29°42'6.9"S; 53°47'28.5"W), both in outskirts of Santa Maria (Huene 1942; Langer *et al.* 2007). Schultz (1991) and Langer (1996) referred a partial dentary from 'Cerro da Alema' to '*S.*' *sulcognathus*, but the material has no diagnostic traits of the taxon. Contreras & Bracco (1989) suggested the presence of '*S.*' *sulcognathus* in the Ischigualasto Formation (Carnian, Late Triassic) of Argentina. Yet, first hand inspections (FCM February 2006) of the MCNSJ collections (where the material is supposedly deposited) revealed no specimens referable to this taxon.

In Linha Facão, specimens were collected somewhat above strata that bore the *Hyperodapedon sanjuanensis* described by Azevedo (1984). Those from Faixa Nova, come from just above a conglomeratic facies that covers a succession of siltstones, in which *Hyperodapedon*, dinosaur, aetosaur, and cynodont remains were collected. The single specimen from Waldsanga was recovered from its conglomeratic facies (Langer 2005), which lies above rhynchosaur-, dinosaur- and cynodont-bearing siltstones, and is covered by a succession of sandy lithofacies. Langer *et al.* (2007) attributed all those deposits to the upper part of the highstand system tract of Santa Maria Sequence 2 (*sensu* Zeffass *et al.* 2003) that represents the lower part of the Caturrita Formation (Andreis *et al.* 1980). Biochronological studies (Langer *et al.* 2007) suggest an early Norian age for these beds.

**Institutional abbreviations.** BMNH: Natural History Museum, London, England; BRSUG: Department of Earth Sciences, University of Bristol, Bristol, England; BSPHG: Bayerische Staatssammlungen für Paläontologie und Historische Geologie, Munich, Germany; EX: Exeter Museum, Exeter, England; FZB-PV: Fundação Zoobotânica do Rio Grande do Sul, Porto Alegre, Brazil; IGMPT: Institut und Museum für Geologie und Paläontologie, Tübingen, Germany; IML: Instituto Miguel Lillo, Universidad Nacional de Tucumán, San Miguel de Tucumán, Argentina; ISIR: Indian Statistical Institute, Calcutta, India; MAL L'Université d'Antananarivo, Antananarivo, Madagascar; MACN: Museo Argentino de Ciencias Naturales, Buenos Aires, Argentina; MCNSJ: Museo de Ciencias Naturales, Universidad de San Juan, San Juan, Argentina; MCP: Museu de Ciências e Tecnologia, Pontifícia Universidade Católica, Porto Alegre, Brazil; SAM: South African Museum, Cape Town, South Africa; SHRBM: Shrewsbury Museum, Shrewsbury, England; UFRGS: Instituto de Geociências, Universidade Federal do Rio Grande do Sul, Porto Alegre, Brazil.

## 1. Systematic palaeontology

Diapsida Osborn, 1903

Rhynchosauria (Gervais 1859) Osborn, 1903

Hyperodapedontinae Chatterjee, 1969  
(*nom. trans.* ex Lydekker 1885)

*Teyumbaita* gen. nov.

**Type species.** *Scaphonyx sulcognathus* Azevedo & Schultz, 1987.

**Diagnosis.** Same as for the only known species.

**Derivation of name.** From the Brazilian aborigine Tupi-Guarani language (*Teyú*=lizard and *Mbaitá*=parrot), a reference to the edentulous premaxilla and dentary tips, which resemble a pittacid beak.

*Teyumbaita sulcognathus* (Azevedo & Schultz, 1987)  
(Figs 2–16)

The following synonymy list uses the recommended symbols of Matthews (1973).

- 1982 *Scaphonyx sulcognathus* Azevedo, pp. 8–10, 57, 58, 62, 66, 70, 74, 78, 82; figs 2–7, 9, 10; plates I–IV.
- (?)1984 *Scaphonyx sulcognathus* Azevedo, pp. 71, 73.
- 1985 *Scaphonyx sulcognathus* Barberena *et al.*, p. 26.
- p 1986 *Scaphonyx sulcognathus* Schultz, pp. 12–20, 42, 49, 59, 74, 80, 84, 90, 98, 102, 107, 110–120; figs 3(a), 4–6(d–f), 7(d–e), 8, 9(a–d), 10(a–e), 11 (a, c, e, g), 12(a–d); plates 1–7 [Only UFRGS-PV-0232T specimens].
- v\*1987 *Scaphonyx sulcognathus* Azevedo & Schultz, pp. 109–113; figs 1–2; photos 1–2.
- (?)1987 *Scaphonyx sulcognathus* Azevedo, pp. 115–119.
- (?)1989 *Scaphonyx sulcognathus* Azevedo *et al.*, p. 11.
- 1989 *Scaphonyx sulcognathus* Contreras & Bracco, p. 113 figs A1, B1, C1.
- (?)1990 *Scaphonyx sulcognathus* Azevedo *et al.*, pp. 26–28.
- (?)1990 *Scaphonyx sulcognathus* Schultz & Azevedo, p. 39.
- p 1991 *Scaphonyx sulcognathus* Schultz, pp. 132, 177, 181, 203, 214–216, 251–254; figs 28, 37, 38, 40(b), 44, 45, 51–53 [Except UFRGS-PV-0403T material].
- (?)1991 *Scaphonyx sulcognathus* Fariña, pp. 1–41.
- (?)1993 *Scaphonyx sulcognathus* Benton, p. 693.
- (?)1995 *Scaphonyx sulcognathus* Schultz, p. 26.
- p 1996 *Scaphonyx sulcognathus*, Morfótipo 2, *Teyumbaita sulcognathus* Langer [except UFRGS-PV-0403T specimen], pp. 22, 24, 25, 26, 61, 65, 106, 107, 110–112, 137, 138, 144–153, 162, 163, 167, 168, 171, 180, 181, 185, 187, 193.
- 1999 '*Scaphonyx*' *sulcognathus* Schultz, p. 20.
- 2000a '*Scaphonyx*' *sulcognathus* Langer & Schultz, pp. 633, 635, 636, 640, 644, 646–649, 652.
- 2000b '*Scaphonyx*' *sulcognathus* Langer & Schultz, pp. 261, 263; figs 9(d), 10.
- 2000a '*Scaphonyx*' *sulcognathus* Langer *et al.*, pp. 111, 114; figs 4(c), 5(b).
- 2000b '*Scaphonyx*' *sulcognathus* Langer *et al.*, pp. 120, 126; figs 1, 7.
- 2004 '*Scaphonyx*' *sulcognathus* Nesbitt & Whatley, p. 6; fig. 5e.
- 2004 '*Scaphonyx*' *sulcognathus* Barros, p. 39. fig. 11.
- 2005 '*Scaphonyx*' *sulcognathus* Whatley, pp. 6, 12–15, 18, 19, 21, 57, 66, 69, 71, 72, 74, 78, 83, 87, 90, 91, 93–96, 102, 109, 111, 114–116, 118–125, 134, 138, 144, 145, 217–227, 235–242, 245, 246, 248–250, 255.
- 2005 '*Scaphonyx*' *sulcognathus* Langer, pp. 205, 208, 212–215.
- 2007 N.gen. *sulcognathus* Langer *et al.*, pp. 205, 208, 211.
- (?)2008 '*Scaphonyx*' *sulcognathus* Hone & Benton, 106–115.
- 2008 '*Scaphonyx*' *sulcognathus* Montefeltro, pp. 29, 31, 33, 35, 41, 50, 55; figs 3b, 4b, 5b, 8b, 11a, 15b, 18d.
- 2008 '*S.*' *sulcognathus* Montefeltro & Langer, pp. 133–135.

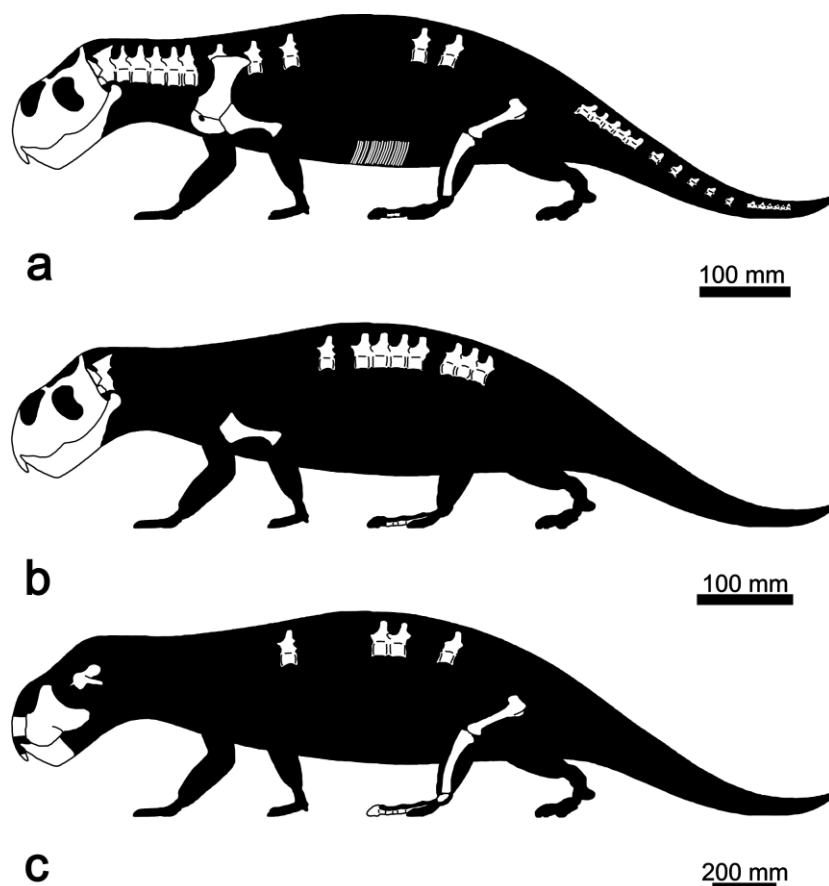


**Figure 2** Schematic outlines of the three more complete specimens of *Teyumbaita sulcognathus*: (a) Holotype (UFRGS-PV-0232T); (b) UFRGS-PV-0298T; (c) UFRGS-PV-0290T.

**Holotype.** UFRGS-PV-0232T (Figs 2–9), complete skull, complete mandibles, atlas, axis, and following four cervical vertebrae, four disarticulated trunk vertebrae, sixteen disarticulated caudal vertebrae, partial gastralia, complete left scapulocoracoid, partial right scapulocoracoid, left humerus, right femur, right tibia, and two isolated phalanges.

**Referred specimens.** UFRGS-PV-0298T (Figs 2, 10–13), almost complete skull, complete right mandible, posteriormost and anteriormost parts of left mandible, axis, four trunk centra, further unprepared trunk centra and neural arches, rib fragments, left humerus, distal portion of the right humerus, two isolated metapodials, and four articulated phalanges; UFRGS-PV-0290T (Figs 2, 14–16), partial skull including right jugal, fragmentary premaxilla, both maxillary plates, and almost complete neurocranium, two articulated and two disarticulated trunk vertebrae, right femur and tibia, proximal part of the right fibula, right astragalus, nine phalanges; UFRGS-PV-0418T, two fragments of a right mandible; UFRGS-PV-0420T, fragmentary right dentary, and unidentified postcranial materials; UFRGS-PV-0445T, partial maxilla; MCP-683, partial left dentary.

**Diagnosis.** Rhynchosaur with anterior margin of nasal concave at midline, prefrontal separated from the ascending process of the maxilla, palatal ramus of pterygoid expanded laterally within palatines, dorsal surface of exoccipital markedly depressed, and a single tooth lingually displaced from the main medial tooth-bearing area of the maxilla.

## 2. Description

The following description is based on the holotype of *Teyumbaita sulcognathus* (UFRGS-PV-0232T) and the two more

complete specimens referred to the taxon (UFRGS-PV-0298T and PV-0290T), but differences among specimens are highlighted when necessary. Figure 2 shows a schematic illustration of the preserved parts of the three specimens.

### 2.1. Skull (Figs 3–7, 10, 11, 14, 15)

**2.1.1. General description.** Both nearly complete skulls (UFRGS-PV-0232T and PV-0298T) show a delicate construction compared to other Hyperodapedontinae, and skull measurements (Table 1) indicate an average size (Huene 1942; Sill 1970; Chatterjee 1974; Benton 1983; Langer & Schultz 2000a). On the other hand, based on the dental plates and neurocranium, UFRGS-PV-0290T is larger and more robust than the other specimens of *T. sulcognathus*.

The holotypic skull is dorso-ventrally compressed (Figs 3–5), whereas UFRGS-PV-0298T shows postero-lateral compression on its left side (Fig. 10), with the ventral ramus of the squamosal displaced antero-medially. These distortions influence major skull measurements (midline length, maximum skull width, and maximum skull height). However, the typical rhynchosaur dorsal triangular shape is retained in all specimens and, as in other Hyperodapedontinae, the skulls are broader than long and higher than half of their length. Likewise, the general dorsal orientation of the orbits is not affected (Fig. 14).

#### 2.1.2. Dermal bones of the skull roof.

**2.1.2.1. Premaxilla.** The paired premaxillae are dorso-ventrally oriented and toothless; these features are considered apomorphic for Rhynchosauria and Rhynchosauridae respectively (Langer 1996; Dilkes 1998; Hone & Benton 2008). They are more anteriorly bowed in UFRGS-PV-0232T than in UFRGS-PV-0298T, a possible taphonomic distortion. The

**Table 1** Skull measurements of the holotype (UFRGS-PV-0232T) and the two more complete specimens of *Teyumbaita sulcognathus* (in cm). The maximum skull height was measured from the maxillary ventral border to the prefrontal ridge.

	UFRGS-PV-0232T	UFRGS-PV-0298T	UFRGS-PV-0290T
Skull midline length	13.5	12.1	–
Maximum skull width	25.7	15.8	–
Maximum skull height	9.3	12.9	–
Maximum width of maxillary tooth bearing area (left)	3.5	3.5	–
Maximum width of maxillary tooth bearing area (right)	3.5	3.6	5.6
Maxillary tooth bearing area length (left)	10.1	7.9	13.6
Maxillary tooth bearing area length (right)	10	9.1	13.1
Mandible length (left)	22.8	–	–
Mandible length (right)	22.9	24	–
Mandible depth at the coronoid (left)	5.5	–	–
Mandible depth at the coronoid (right)	5.3	6.9	–

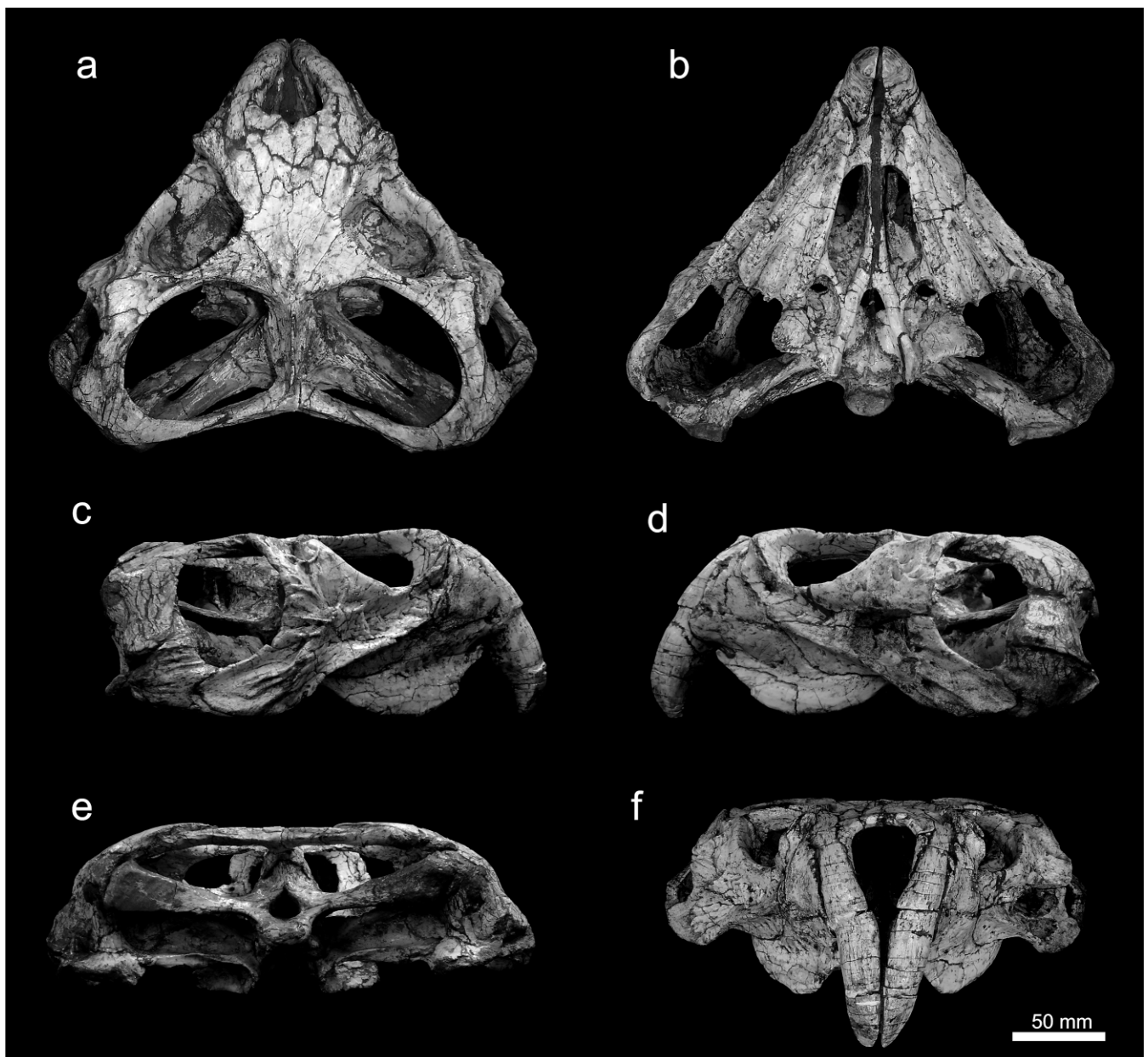


**Figure 3** *Teyumbaita sulcognathus*, holotype skull (UFRGS-PV-0232T): (a) dorsal view; (b) ventral view; (c) right lateral view; (d) left lateral view; (e) occipital view; (f) anterior view.

proximal surface of each premaxilla fits into a notch formed by both vomer and maxilla, and extends dorsally onto a groove formed by lacrimal, nasal and prefrontal. In UFRGS-PV-

0232T, because the left proximal premaxillary tip is missing, the groove is more evident. Dorsally, the premaxillae are separated by the single external naris, but they converge

ventrally to meet one another in an unsutured symphysis, i.e., forming the apomorphic rhynchosaurid ‘beak’. In this area, each premaxilla reaches its greatest breadth, and has an approximately triangular cross-section, with a flattened medial face. The premaxillae of UFRGS-PV-0290T are fragmentary. Two more complete pieces represent a median segment from the right bone and the distal tip of left one. The median segment seems more laterally compressed than in UFRGS-PV-0232T and UFRGS-PV-0298T.

**2.1.2.2. Nasal.** The nasal pair is longer than broad. Its anterior margin forms the posterior border of the single median external naris. Each bone sends an antero-lateral extension that overlaps the premaxilla medially, following its curvature to reach the ascending process of the maxilla. The nasal pair (UFRGS-PV-0232T and UFRGS-PV-0298T) is autapomorphic on its concave anterior margin at the midline. The articulation to the prefrontal forms an oblique line, and that to the frontal is ‘U’- shaped, with the concavity directed posteriorly.

**2.1.2.3. Frontal.** The frontal pair forms the interorbital region of the skull roof. Each bone is subtriangular, with a more laterally expanded median region and narrowing anterior and posterior ends. Their lateral tips border the orbits for a short distance. The medial suture of the pair is irregular, bearing a ridge on the posterior third. Unlike *H. gordonii*, *H. huenei*, and some South American *Hyperodapedon* specimens (e.g.: IMGPT-19-2), the frontal crest is not continuous with the sagittal crest. Lateral to the crest, each frontal bears an antero-posteriorly oriented shallow groove that, unlike most *Hyperodapedontinae* (except some Argentinean *Hyperodapedon* specimens, e.g.: IML-3432), is deeper posteriorly. The presence of a frontal depression was first considered a rhynchosaur apomorphy (Dilkes 1995, 1998), whereas later works (Langer & Schultz 2000a; Hone & Benton 2008) accounted for depth differences among taxa. In fact, frontal depressions not posteriorly deeper seem diagnostic for *Hyperodapedon*, consequently excluding *T. sulcognathus* from that genus (Langer & Schultz 2000a).

Each frontal is antero-laterally overlapped by the respective prefrontal. Postero-laterally, it contacts the postfrontal along a ridged oblique suture. The ridge is not conspicuous, but more evident in the middle of the suture. It is not continuous with the sagittal crest as in *Stenaulorhynchus stockleyi* (Haughton 1932), the new skull of *Fodonyx spenceri* (Hone & Benton 2008), and the specimen informally known as ‘Rincossauro de Mariante’ (Schultz & Azevedo 1990). Anterior processes of the parietal overlap the posterior margin of the frontals laterally, differing from the interdigitated articulation described for *H. gordonii* and *H. huenei* (Benton 1983; Langer & Schultz 2000a).

**2.1.2.4. Parietal.** The fused parietals form the typical T-shaped element of rhynchosaurids, with a single anterior ramus and two laterally-diverging wings at the posterior end. The anterior ramus forms the intertemporal bar and bears a prominent sagittal crest that does not reach the anterior and posterior tips of the bone. Anteriorly, this ramus becomes wider and is firmly attached to the frontals and postfrontals. Ventrally, it has a slot that overlaps the supraoccipital and opisthotic dorso-laterally. The parietal also articulates with the postorbital via short, diverging antero-lateral processes that take only small parts in the antero-medial border of the upper temporal fenestra. This contact is hidden by the postfrontal in dorsal view (Fig. 4a).

Similar to the condition in *Fodonyx spenceri* (Hone & Benton 2008) and all other Late Triassic rhynchosaurs, the posterior wings of the parietal of *T. sulcognathus* are directed laterally, rather than postero-laterally, as in the Middle Triassic rhynchosaurs. Each wing meets the medial process of the

squamosal laterally. In UFRGS-PV-0298T, a ridge extends along the dorsal margin of the wings. In the holotype, possibly due to its dorso-ventral compression, the ridge occupies the posterior surface of the wings, and is mainly visible in occipital view (Fig. 5b).

**2.1.2.5. Lacrimal.** The lacrimal is a small and robust element that takes part in the orbital margin. In dorsal view (Fig. 4b), this bone forms most of the protruding anterior border of the orbit, which is mainly formed by the prefrontal in other *Hyperodapedontinae* (Langer & Schultz 2000a; Whatley 2005). In any case, such a protruding orbital margin is apomorphic for that group. In lateral view (Fig. 4b), the lacrimal contacts the maxilla anteriorly, the jugal postero-ventrally, and is posteriorly overlapped by the descending process of prefrontal. The maxilla–lacrimal suture follows the curvature of the orbital rim and is continuous to the jugal–maxilla articulation. In medial view (Fig. 4a), the anterior and ventral margins of the lacrimal are sutured to the descending process of the prefrontal, while its posterior margin articulates to the jugal. In the inner surface of the orbit, the contact between lacrimal and the ascending process of the palatine is not clearly seen, but the medial surface of the bone is pierced by two foramina of the lacrimal duct.

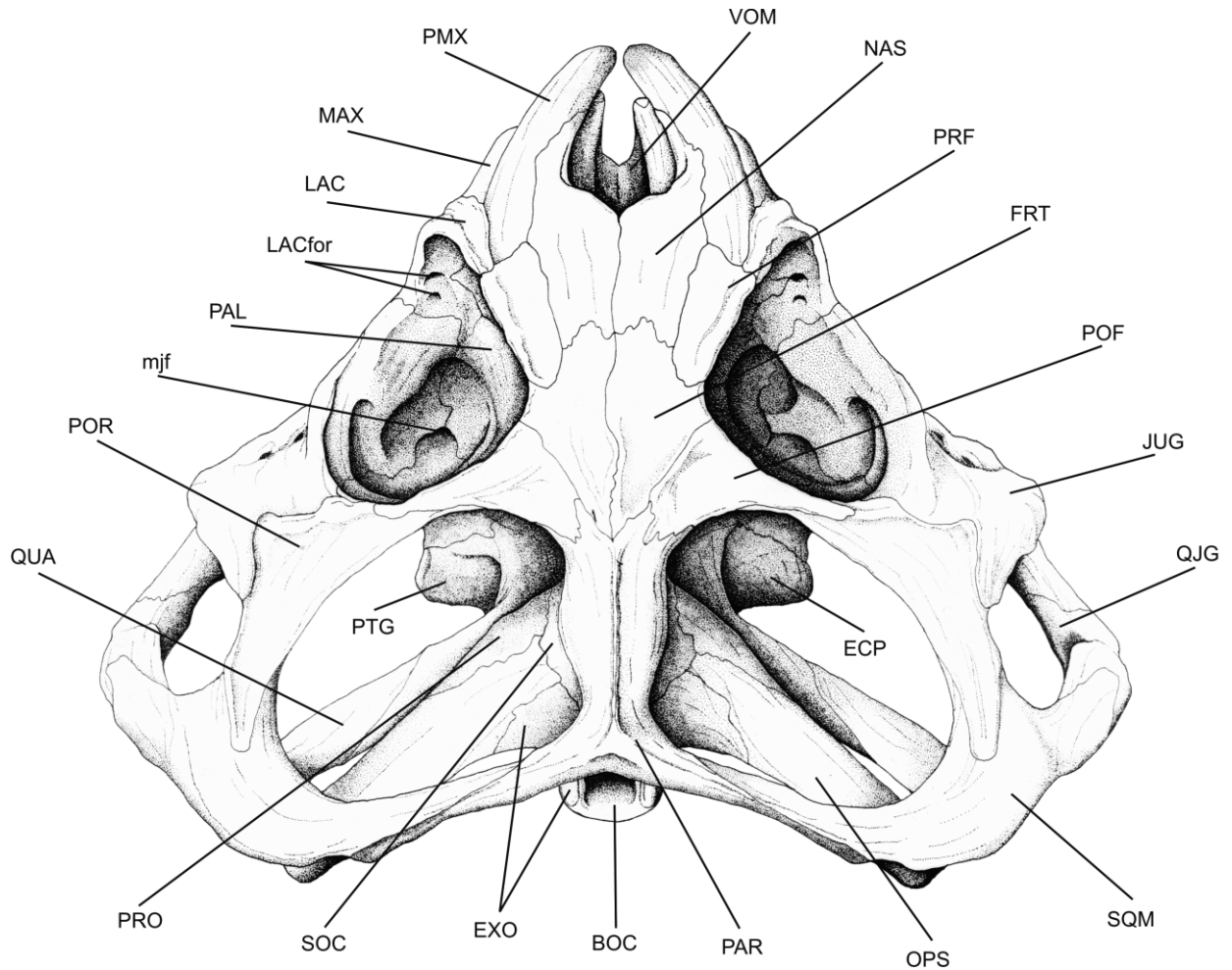
**2.1.2.6. Prefrontal.** The prefrontal is subrectangular in dorsal view and forms, together with the lacrimal, the protruding anterior orbital rim. Yet, it only forms a small part of the orbital margin, and does not meet the ascending process of maxilla; an autapomorphy of *T. sulcognathus*. The ventral portion of the bone forms most of the antero-medial orbital cavity and meets the ascending process of palatine in an almost vertical ridge. Its posterior margin is extended, apparently setting the lacrimal and the ascending process of the palatine apart.

**2.1.2.7. Postfrontal.** The postfrontal is a three-pronged element that forms the postero-medial margin of the orbit and the anterior border of the upper temporal fenestra. Its dorsal surface bears a shallow depression, but does not show the pitted sculpture advocated as an apomorphy of Rhynchosauria (Dilkes 1995, 1998; Hone & Benton 2008). The tongue-like lateral ramus is firmly attached to a dorsal depression of the postorbital medial process, and hides the contact between the parietal and the postorbital on anterior margin of the upper temporal fenestra.

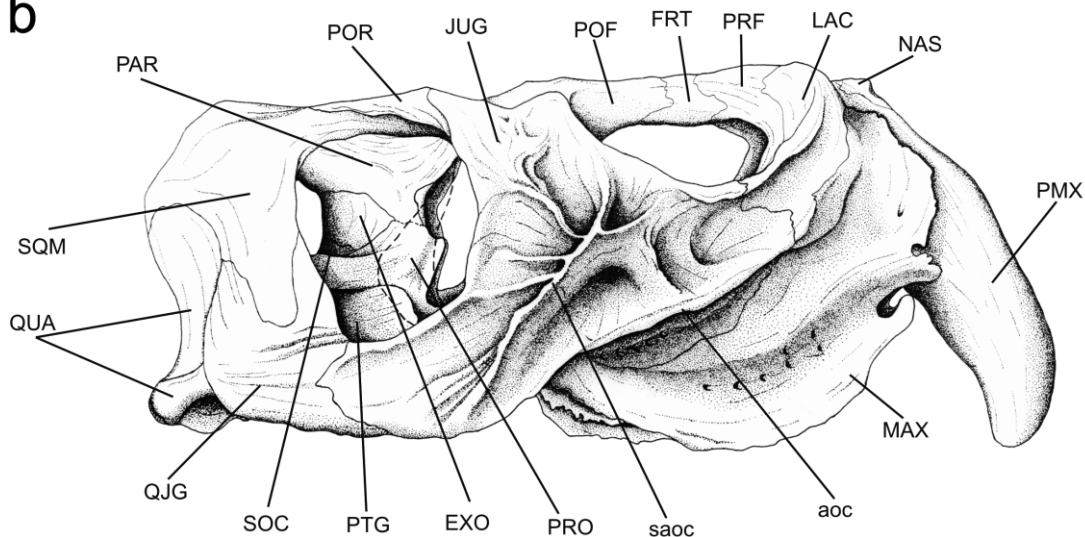
**2.1.2.8. Postorbital.** This tri-radiated element forms part of the borders of the orbit, upper, and lower temporal fenestrae. Its posterior process is longer than the ventral, unlike Early Triassic forms in which the reverse is the case (Dilkes 1998; Hone & Benton 2008). In all *T. sulcognathus* specimens, the ventral process attaches firmly to the dorsal margin of the ascending process of the jugal, as in *Hyperodapedon*, and is not anteriorly overlapped by that structure, as in more basal taxa. The posterior process overlaps the antero-dorsal process of the squamosal, and forms the external surface of the intertemporal bar. The medial process forms a robust orbital rim, analogous to that of the lacrimal, prefrontal and jugal. In posterior view (Fig. 5b), the suture of this process to the parietal takes place at the medial third of the anterior edge of the upper temporal fenestra. A few depressions are seen on the middle and posterior surface of the bone.

**2.1.2.9. Jugal.** The jugal is a large and complex triradiated element that occupies most of the lateral skull surface. The anterior ramus forms most of the ventral border of the orbit. It contacts the lacrimal anteriorly, and the maxilla ventrally in a long curved articulation that is continuous with that of lacrimal-maxilla. The anterior ramus laterally overlaps the posterior portion of the tooth-bearing area of maxilla. The external surface of that ramus has a well-marked *anguli oris*

a



b



c

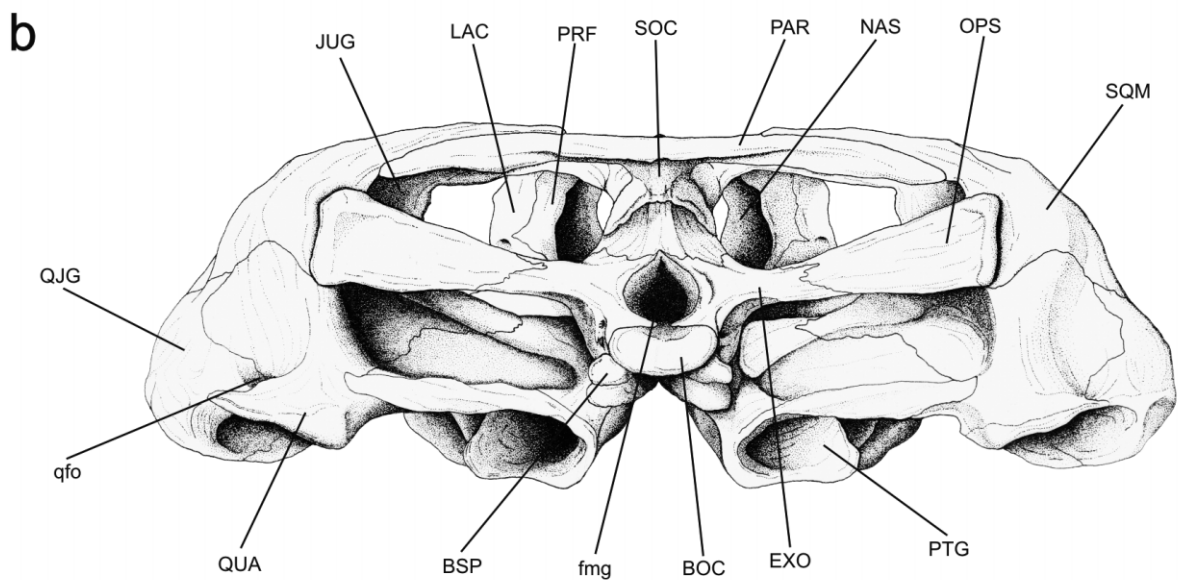
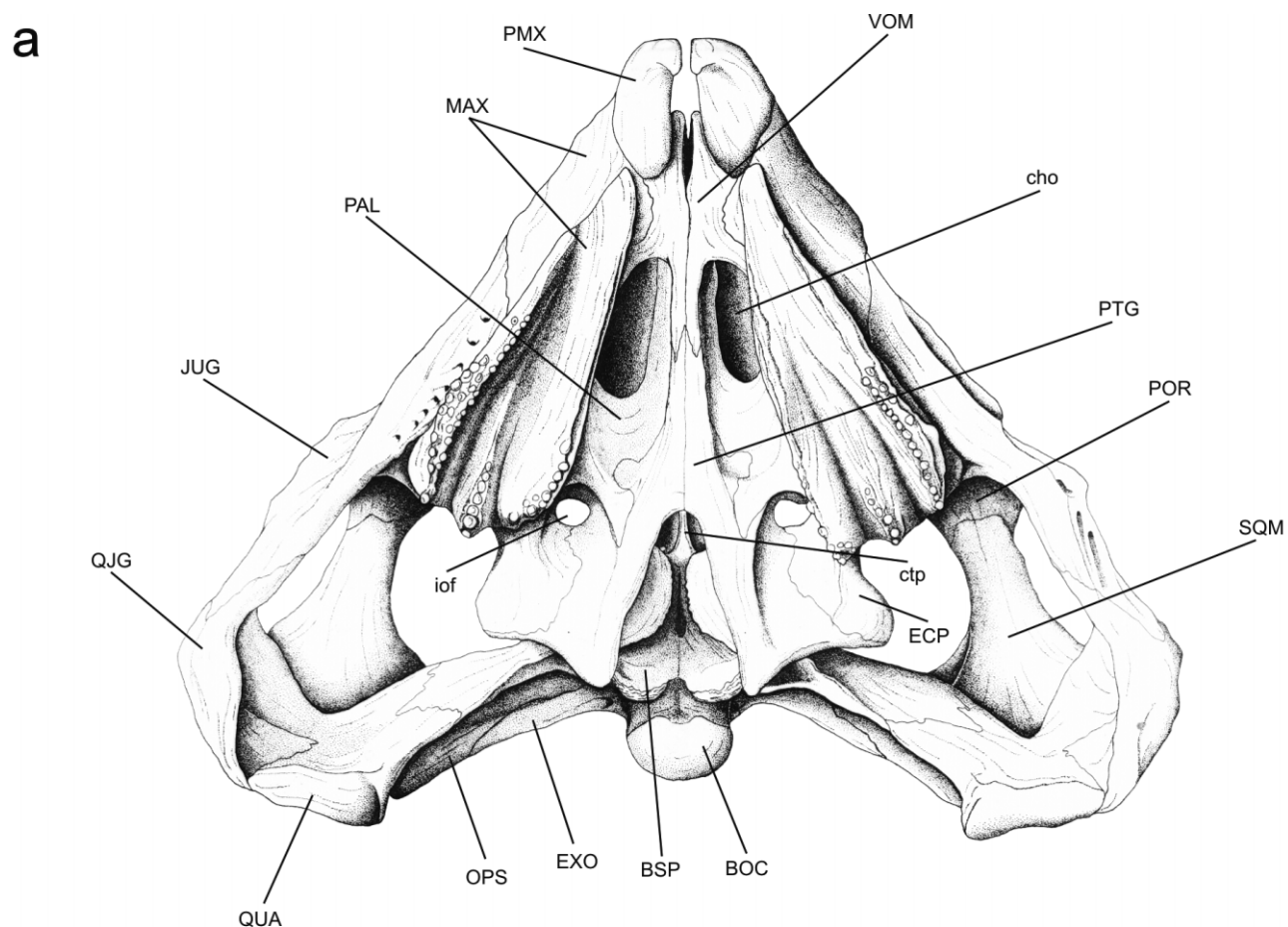


50 mm

**Figure 4** *Teyumbaita sulcognathus*, holotype skull (UFRGS-PV-0232T) modified from Azevedo (1982): (a) dorsal view; (b) right lateral view, dashed lines indicate the original position of the epipterygoid; (c) right epipterygoid lateral view. Abbreviations: aoc=anguli oris crest; BOC=basioccipital; ECP=ectopterygoid; EXO=exoccipital; FRT=frontal; JUG=jugal; LAC=lacrimal; LACfor=lacrimal foramens; MAX=maxilla; mjf=medial jugal foramen; NAS=nasal; OPS=opisthotic; PAL=palatine; PAR=parietal; PMX=premaxilla; POF=postfrontal; POR=postorbital; PRF=prefrontal; PRO=pro-otic; PTG=pterygoid; QJG=quadratejugal; QUA=quadrate; saoc=secondary anguli oris crest; SOC=supraoccipital; SQM=squamosal; VOM=vomer.

crest, which begins in the posterior portion of the jugal–maxilla contact and extends (as an extension of the ventral border of the postero-ventral ramus) antero-dorsally along the entire length of the ramus. It reaches the anterior end of the

jugal and does not extend anteriorly along the posterior portion of the maxilla–lacrimal articulation, as also seen in *Hyperodapedon gordonii* and *H. huxleyi*, but not in *H. huenei* (Langer & Schultz 2000a). Such a well-developed *anguli oris*



50 mm

**Figure 5** *Teyumbaita sulcognathus*, holotype skull (UFRGS-PV-0232T) modified from Azevedo (1982): (a) ventral view; (b) occipital view. Abbreviations: BOC=basioccipital; BSP=basisphenoid/parasphenoid; cho=choana; ctp=cultriform process; ECP=ectopterygoid; EXO=exoccipital; fmg=foramen magnum; iof=inferior orbital foramen; JUG=jugal; LAC=lacrimal; MAX=maxilla; NAS=nasal; OPS=opisthotic; PAL=palatine; PAR=parietal; PMX=premaxilla; POR=postorbital; PRF=prefrontal; PTG=pterygoid; qfo=quadrate foramen; QJG=quadrate foramen; QUA=quadrate; SOC=supraoccipital; SQM=squamosal; VOM=vomer.

crest is typical of hyperodapedontines. Other rhynchosaurs, on the contrary, have a shorter crest that is restricted to the posterior part of the anterior jugal process (Chatterjee 1974; Benton 1983, 1990; Langer & Schultz 2000a). The row of foramina that occurs below this crest in *H. gordonii* and *H. huxleyi* (Chatterjee 1974; Benton 1983; Langer & Schultz 2000a) is also present in *T. sulcognathus*. The inner surface of the anterior jugal process bears an oblique crest that extends in roughly the same direction as the external *anguli oris*. As in *H. huenei*, this crest is more pronounced antero-dorsally, where the jugal attaches to the lacrimal (Langer & Schultz 2000a). Ventral to that suture, and in contrast to the situation seen in *H. huenei* (Langer & Schultz 2000a), the jugal bears no descending ridge, but the canal extending between the anterior part of the bone and the ascending process of the palatine (infraorbital foramen *sensu* Benton 1983) is present, as in *H. gordonii* and *H. huxleyi* (Chatterjee 1974; Benton 1983). Posterior to this canal, the jugal has an almost horizontal surface that overlaps the maxilla and forms the ventro-lateral floor of the orbit cavity. The antero-medial contact of that surface with the vertical ridge of the palatine is not clear, but the posterior part of the suture is preserved. Postero-medially, the jugal contacts the dorso-lateral process of the ectopterygoid, forming a well-marked vertically-oriented ridge. As in *H. gordonii* and *H. huenei*, the medial jugal foramen pierces the palate where jugal, palatine and ectopterygoid are in contact.

The dorsal process of the jugal forms the main part of the bar between the orbit and the lower temporal fenestra. It is wider than 40% of the total orbital opening, as in all other Hyperodapedontinae. Dorsally, this process is firmly attached to the ventral process of the postorbital, but in contrast to *H. gordonii* (Benton 1983), *H. huenei* (Langer & Schultz 2000a) and *H. mariensis* (FZB-PV-1867), it does not contact the squamosal. The same condition is seen in *H. huxleyi* (Chatterjee 1974) and some South American specimens of *Hyperodapedon*, e.g., MCNSJ-680, UFRGS-PV-0262T, UFRGS-PV-0408T, UFRGS-PV-0149T. The sickle-shaped postero-ventral process of the jugal forms most of the ventral edge of the lower temporal fenestra. This process overlaps the anterior process of the quadratojugal laterally. In UFRGS-PV-0298T, the dorsal margin of the anterior process of the quadratojugal is better seen than in the holotype and UFRGS-PV-0290T, in which it is covered by the jugal.

The external surfaces of the dorsal and postero-ventral processes of the jugal bear a complex pattern of sculpture. Langer & Schultz (2000a) recognised that hyperodapedontines and the taxon later named as *Fodonysx spenceri* (Benton 1990) have a jugal ornamented with crests or elevations dorsal to the *anguli oris* crest. Indeed, the holotype of *T. sulcognathus* has an evident secondary *anguli oris* crest, dorsal to the first one, extending from the base of the postero-ventral process to near the ventral orbital edge. A series of radiating ridges and small crests is also visible in the jugal of this specimen. UFRGS-PV-0298T and PV-0290T also possess a secondary *anguli oris* crest, but their locations and extents are different. UFRGS-PV-0298T has a short crest that starts at the dorsal part of postero-ventral process and reaches the middle of the jugal. The radiating ridges and small crests are less developed in this specimen, but more evident between the *anguli oris* crests. UFRGS-PV-0290T, on the other hand, possesses a more common condition, also found in other Hyperodapedontinae, such as *Isalorhynchus genovefae* (Whatley 2005) and some South American *Hyperodapedon* specimens, e.g., BSPHG-18.4. It has a wider, but blunter crest that does not extend anterior to the postero-ventral process. Additionally, radiating ridges and small crests are lacking.

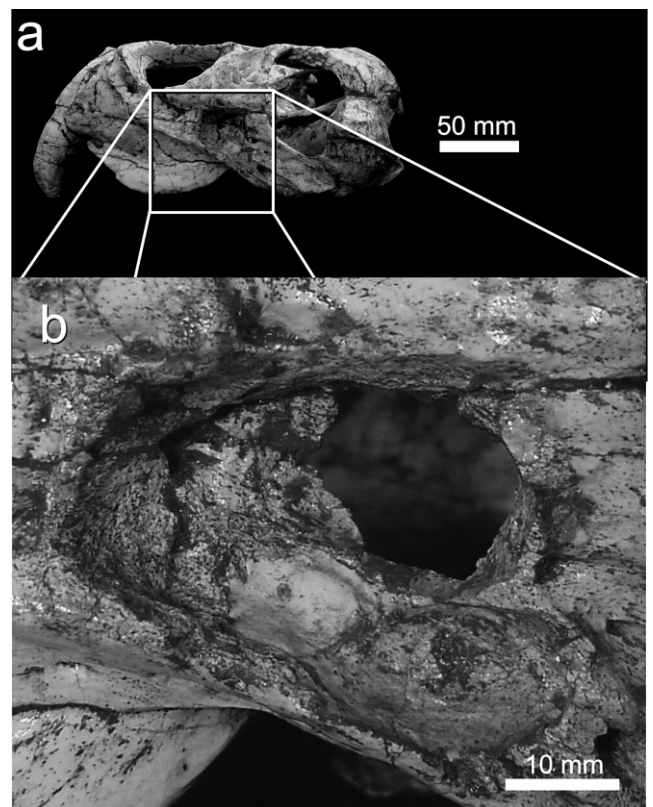


**Figure 6** *Teyumbaita sulcognathus*, holotype skull (UFRGS-PV-0232T): (a) left lateral view; (b) lateral view of the central area of the left jugal, showing the inner structures of the bone.

In the left jugal of the holotype, the medial and, especially, lateral surfaces are missing in the central portion of the bone (Fig. 6). This reveals a complex inner structure, composed of a larger cavity separated by bone septa from three smaller antero-ventral cavities. This abnormality may represent the expression of a pathology affecting a sinus not externally visible otherwise (Schultz 1999).

**2.1.2.10. Quadratojugal.** The quadratojugal is an L-shaped element occupying the postero-ventral corner of the skull. It bears stout dorsal and antero-ventral processes, as in other mid Late Triassic rhynchosaurids. The dorsal process bifurcates dorsally enclosing the descending ramus of the squamosal. The anterior part of this process forms the ventral half of the posterior border of the lower temporal fenestra. In UFRGS-PV-0232T, the posterior part is as long as the anterior, but half the size in UFRGS-PV-0298T. The antero-ventral process forms the medial surface of the lower temporal bar in its posterior half, where it is overlapped externally by the jugal. In occipital view (Fig. 5b), the quadratojugal meets the quadrate medially. This vertical articulation approaches the quadrate condyle at its lateral tip, and bears the quadrate foramen in its ventral portion.

**2.1.2.11. Squamosal.** The squamosal is a triradiate bone that forms much of the postero-dorsal corner of the skull and the temporal openings. In lateral view (Fig. 4b), the anterior process extends under the postero-dorsal process of the postorbital, occupying most of the dorsal edge of the lower temporal fenestra. The medial process overlaps the lateral wing of the parietal and forms part of the postero-lateral margin of the upper temporal fenestra. The broad ventral process forms the dorsal half of the posterior edge of the lower temporal fenestra. Ventrally, this part of the bone also extends over the quadrate to reach the dorsal process of the quadratojugal. In occipital view, the squamosal has an expanded medial ramus that bears a medial depression for the paroccipital process, and

firmly holds the dorsal part of the quadrate. In the holotype, this ramus forms a small part of the latero-dorsal corner of post-temporal fenestra, but its contribution to the post-temporal fenestra is greater in UFRGS-PV-0298T.

### 2.1.3. Dermal bones of the palate.

**2.1.3.1. Maxilla.** The maxilla is composed of a robust body, its ventral face bearing teeth, and a thin antero-lateral ascending process (Fig. 5a). The medial surface of the ascending process forms most of the lateral wall of the nasal cavity, whereas its lateral surface contacts the lacrimal and the anterior process of the jugal ventrally. Its anterior edge overlaps the dorsal half of the premaxilla laterally. At the base of this process, the anterior margin of the maxilla has a small hook-shaped notch, the same element is seen in *H. huenei* (Whatley 2005) and considered here a modification of that found in most mid Late Triassic rhynchosaurs (Langer & Schultz 2000a). Just below the *anguli oris* crest the lateral maxillary surface of UFRGS-PV-0232T and UFRGS-PV-0298T shows a series of small nervous and vascular openings, which are not evident in UFRGS-PV-0290T.

The robust maxillary body is antero-medially to postero-laterally oriented. The tooth-bearing area is ventrally convex and broader posteriorly, with straight margins in UFRGS-PV-0232T and PV-0298T. On the contrary, the maxillary plates of UFRGS-PV-0290T have convex medial and concave lateral margins. The ventral maxillary surface is composed of three tooth-bearing areas separated by two longitudinal grooves into which the dentary blades abut during occlusion. Along its medial margin, the dorsal portion of the maxillary body receives the vomer anteriorly and the palatine and ectopterygoid posteriorly. Between these articulations, the maxilla forms part of the lateral border of the choana. Anteriorly, the dorsal surface of the maxilla forms most of the floor of the nasal cavity. Posteriorly, parts of this dorsal surface are overlapped by the palatine (antero-medially), medial projections of the jugal (laterally), and the dorso-lateral process of the ectopterygoid (postero-medially). In this area, a groove extends between the postero-dorsal margin of the maxilla and the overlapping portions of the jugal and ectopterygoid. Because the postero-ventral process of the ectopterygoid covers the postero-medial corner of the dental plate, extending anteriorly to contact the palatine, the maxilla is excluded from the margin of the inferior orbital foramen.

**2.1.3.2. Vomer.** Each vomer is composed of an antero-posteriorly directed medial body, and a lateral process extending from its anterior portion. The anterior margin of the pair is V-shaped for the reception of the pre-maxillae. In contrast to the condition seen in *H. gordonii*, *H. huxleyi*, and *H. huenei*, the anterior parts of the vomers are not fused at the midline. Each bone forms the anterior border of the choana, and meets the palatal ramus of the pterygoid posteriorly, half-way along the choanal extension, and touching the palatine latero-dorsally. On the other side of the choana, the lateral process of the vomer forms its antero-lateral border, and is attached to the antero-medial surface of the maxilla. The dorsal surface of the vomer forms the bottom of the nasal cavity, where no good evidence of a low medial crest, proposed to support cartilages of the narinal septum (Langer & Schultz 2000a), is seen.

**2.1.3.3. Palatine.** As in other hyperodapedontines, the palatine of *T. sulcognathus* does not contact its pair at any point. It forms the medial part of the orbital floor, contacting the descending ridge of prefrontal antero-laterally, and possibly the lacrimal. The putative limits between these bones are not clear at the base of the prefrontal ridge, but the palatine extends posteriorly to touch the jugal near the medial jugal foramen. It also contacts the ectopterygoid posterior to the medial jugal foramen.

In ventral view (Fig. 5a), the anterior portion of the palatine bears a plate-like process that contacts the vomer anteriorly, overlaps the anterior process of the pterygoid laterally, outlines the dorsal part of the medial surface of the choana, roofs the posterior part of the internal naris, and forms the greatest part of the choanal fossa. At its posterior portion, the bone forms a ridged lateral extension that overlaps the postero-medial portion of the maxilla and contacts the ectopterygoid medially to the inferior orbital foramen. At its medial contact with the pterygoid, the palatine is overlapped by a small lateral concealed expansion of that bone.

**2.1.3.4. Pterygoid.** The pterygoid is a complex element forming most of the posterior palate. Each bone has an antero-posteriorly-directed palatal ramus and two laterally-directed processes on its posterior portion (ectopterygoid and quadrate processes). The antero-posteriorly-directed palatal ramus meets its pair medially, contacts the blade-like process of the palatine dorso-laterally, and firmly attaches to the vomer anteriorly to form the ventro-medial portion of the choanal opening. The posterior portion of the palatal ramus descends under the neurocranium, forming two lateral branches that delimit a narrow interpterygoid vacuity. In dorsal view (Fig. 4a), this ramus extends laterally, forming the medial portion of the posterior border of the orbital cavity. The palatal ramus has an autapomorphic concealed lateral expansion entering the palatine. Postero-dorsally, the palatal ramus bears a stout dorsal process for the reception of the basiptyergoid process of the basisphenoid/parasphenoid.

The ectopterygoid process of the pterygoid expands laterally from the posterior portion of the palatal ramus. Its entire lateral portion is ventrally overlapped by the ectopterygoid, which also overlaps its antero-lateral surface dorsally. The quadrate process is a thin sheet of bone, well developed dorso-ventrally, with ridged edges and a deep concavity on its posterior surface. It extends postero-laterally from the articulation between the posterior edge of the palatal ramus and the neurocranium. Its medial surface articulates ventrally with the basisphenoid/parasphenoid, and anteriorly to the basal portion of the epipterygoid and the ventral part of the pro-otic. Laterally, the process overlaps the pterygoid process of the quadrate. In contrast to all other Late Triassic rhynchosaurs, the quadrate process of *T. sulcognathus* does not meet the ventral margin of the paroccipital process.

**2.1.3.5. Ectopterygoid.** The ectopterygoid is a small element restricted to the latero-posterior portion of the palate, which bears postero-ventral and dorso-lateral processes. The postero-ventral process overlaps the lateralmost part of the ectopterygoid process of the pterygoid ventrally, extending far posterior beyond that process. It fits against the postero-ventral border of the maxilla, contacting the palatine at the medio-posterior corner of the maxillary plate, lateral to the inferior orbital foramen. The dorso-lateral process is more complex, antero-dorsally overlapping that same pterygoid process, and extending forward to meet palatine and jugal dorso-laterally. Anteriorly, this dorso-lateral process has a prominent buttress that forms the posterior borders of both the orbital cavity and the inferior orbital foramen.

### 2.1.4. Quadrate and epipterygoid.

**2.1.4.1. Quadrate.** The quadrate occupies the latero-ventral corner of the skull and does not project posteriorly to the occiput. Three main parts compose this bone, the columnar body, the medial process, and the condylar surface. The body is a robust structure overlapping the ventral part of the squamosal dorsally and the medial portion of the posterior surface of the quadratojugal laterally. It bears a well-marked pillar-like central portion (posterior crest *sensu* Benton 1983) that extends along its entire dorso-ventral length with a

median smooth constriction, also seen in other *Hyperodapedontinae*. The quadrate foramen pierces the ventral portion of the quadrate–quadratojugal suture. Medial to the columnar body, the quadrate has a thinner subtriangular medial process that meets the quadrate ramus of the pterygoid in an irregular suture. This process is more dorsally developed than in *H. gordonii* and *H. huenei* (Benton 1983; Langer & Schultz 2000a). Moreover, its dorsal margin bears a ridge that is continuous to the ridged dorsal edge of quadrate process of the pterygoid. The medio-laterally directed condylar surface is located ventrally to the columnar body. This is inclined in relation to the palatal plane, with the medial portion more ventrally projected. The two fields of condylar surface of *H. gordonii* are also seen in holotype of *T. sulcognathus*, but not in UFRGS-PV-0298T, perhaps due to the better preservation of the former.

**2.1.4.2. Epipterygoid.** The holotypic right epipterygoid was preserved isolated from the skull and its position was inferred based on comparison with other taxa. The epipterygoid has a thin subtriangular base and a rod-like ascending process. This bone probably lay lateral to the neurocranium, with the ventral portion of the plate-like base applied to the dorsal portion of the antero-medial margin of the quadrate process of the pterygoid. As in *H. gordonii* and *H. huenei* (Benton 1983; Langer & Schultz 2000a), its dorsal portion presumably overlapped the anterior area of the suture between the prootic and basisphenoid/parasphenoid, whilst the ascending process would have bordered the antero-lateral surface of the prootic and supraoccipital. A dorsal contact with the parietal is also inferred based on comparison with *H. huenei*.

#### 2.1.5. Neurocranium. (Figs 7, 11, 15)

**2.1.5.1. Supraoccipital.** The supraoccipital is a single median pillar-like element, the base of which forms a small part of the dorsal edge of the *foramen magnum* and the roof of the brain cavity. In occipital view, its ventral region contacts the exoccipital pair, but its anterior part is also attached to the opisthotics postero-ventrally and prootics antero-ventrally by means of ventro-lateral projections. Dorsally, the supraoccipital fits into a well-marked concavity on the ventral surface of the parietal.

**2.1.5.2. Exoccipital.** Each exoccipital possesses a plate-like ventro-medial process that forms the postero-lateral surface of the braincase and a lateral process that forms the postero-proximal region of the paroccipital process. In the holotype, the exoccipital pair forms the almost the entire margin of the *foramen magnum*, except for its dorsalmost and ventralmost portions, formed by the supraoccipital and basioccipital respectively. In both the holotype and UFRGS-PV-0290T, each ventro-medial process overlaps the basioccipital dorsally, but does not reach its pair medially. This is also seen in *H. mariensis*, *H. sanjuanensis*, *H. huenei* (*contra* Langer & Schultz 2000a) and *Isalorhynchus* (Whatley 2005), but not in *H. huxleyi* or *H. gordonii* (Chatterjee 1974; Benton 1983). The processes also expand posteriorly, firmly attached to the basioccipital, forming the dorso-lateral portions of the occipital condyle. Each lateral process overlaps the posterior side of the opisthotic and forms the postero-medial part of the paroccipital process. Its ventro-medial surface bears two small hypoglossal foramina. The dorsal surface of the exoccipital is distinctively depressed in an autapomorphic fashion, as seen in both UFRGS-PV-0232T and PV-0290T. This depression occupies the entire dorsal surface of the bone, and its limits are coincident with the exoccipital–opisthotic suture.

**2.1.5.2. Basioccipital.** The basioccipital is a heavily-built, compact bone that expands posteriorly to form the major portion of the single reniform occipital condyle. Its dorsal surface is mostly covered by the exoccipitals, so that it

has little participation in the floor of the neural channel. Anterior to the condyle, the basioccipital is constricted, but at its anterior end it becomes more laterally developed, forming the diverging tubera speno-occipitales that anteriorly meet the basisphenoid/parasphenoid complex. The tubera are better developed in UFRGS-PV-0298T and PV-0290T, and have a rugose surface. The suture between the basioccipital and the basisphenoid/parasphenoid has an oblique orientation in ventral view. It is tangential to the tubera speno-occipitales and converges postero-medially. At this ventral surface, UFRGS-PV-0298T bears two small rounded deep depressions, whereas only one, possibly the anterior, is seen in the other two specimens. In lateral view, the dorso-lateral surface of the bone receives a small ventral process of the opisthotic. Behind that contact, the basioccipital forms the ventral border of the metotic foramen.

**2.1.5.3. Basisphenoid/parasphenoid.** As in other rhynchosaurs, and many archosauromorphs, the basisphenoid and parasphenoid are not differentiated (see Romer 1956; Gower & Sennikov 1996; Dilkes 1998; Gower & Nesbitt 2006; Desojo & Baéz 2007), and are described as a single unit here. This articulates with the anterior surface of the tubera speno-occipitales via two plate-like expansions of its posterior margin. Anterior to those expansions, the paired basiptyergoid processes extend ventrally and contact blunt articular facets of the pterygoid on the dorsal border of the interptyergoid vacuity. These processes are similar to those seen in *Hyperodapedon*, but differ from the slender processes of Middle Triassic rhynchosaurs (Benton 1983) and *Isalorhynchus* (Whatley 2005). The position and form of the articular facets of the basiptyergoid processes vary significantly among the specimens of *T. sulcognathus*. These are almost ventrally oriented in UFRGS-PV-0232T, with their posterior region slightly ventrally displaced, whereas in UFRGS-PV-0298T and PV-0290T, the facets face antero-laterally. This difference could be attributed to the marked dorso-ventral compression of the holotypic skull. The anterior face of the basisphenoid/parasphenoid and the structures of the dorsum sellae are not well seen in any specimen of *T. sulcognathus*, but in UFRGS-PV-0290T the latter structure seems to be represented by two small rounded depressions, just dorsal to the cultriform process.

In UFRGS-PV-0298T and PV-0290T, only the base of the cultriform process is present, while the holotype preserves all but the anteriormost tip of this slender element that divides the interptyergoid vacuity. It extends antero-dorsally, dorso-medial to the pterygoid palatal ramus. The dorsal contact of the basisphenoid/parasphenoid to the opisthotic and prootic appears to follow a straight line as in *H. gordonii* (Benton 1983) and *H. huenei*, and the opisthotic seems to exclude the basisphenoid/parasphenoid complex from the fenestra ovalis in UFRGS-PV-0232T.

**2.1.5.4. Opisthotic.** Together with prootic and exoccipital, the opisthotic forms most of the paroccipital process, which is the lateral expansion of the neurocranium that meets the squamosal in the dorso-lateral corner of the skull. The opisthotic is composed of two distinct portions, a medial part contributing to the lateral wall of the brain cavity, and a lateral expansion participating in the paroccipital process. The medial part of the opisthotic covers the supraoccipital dorsally, and unlike most *Hyperodapedon*, the bone is not fused to the exoccipital posteriorly. Instead, the articulation is clearly visible in occipital and dorsal views of the holotype. It forms a curve in latter view, mainly coincident with the limits of the depression seen in the dorsal surface of the exoccipital. The latero-ventral surface of the opisthotic has a distinct interfenestralis crest that ventrally meets the dorsal surface of the

tubera sphenoccipitales of the basioccipital. This crest forms the posterior border of the otic capsule, bordering the fenestra ovalis posteriorly and the metotic foramen anteriorly. Although the neurocranial openings on UFRGS-PV-0290T are not clearly seen, this crest is especially distinctive in the preserved portion of the right opisthotic of that specimen. It extends laterally at the ventral face of the proximal part of the paroccipital process, delimiting the stapedia canal (*sensu* Benton 1983), which is more posteriorly placed in *H. gordonii* and *H. huenei* (Langer & Schultz 2000a). The proximal part of the opisthotic lateral expansion fits between the prootic anteriorly and the exoccipital posteriorly. Lateral to that, the bone expands dorso-ventrally, composing the entire paroccipital process.

**2.1.5.5. Prootic.** The pro-otic is better preserved in UFRGS-PV-0232T, composing the entire antero-dorsal portion of the neurocranium, including the anterior portion of the lateral wall of the brain cavity. Two distinct portions are seen, a dorso-ventrally oriented body and a lateral extension that participates on the antero-proximal portion of the paroccipital process. The ventral portion of the dorso-ventrally oriented body is difficult to access because it is partially covered by the quadrate process of the pterygoid and sediment. It lies dorsal to the basisphenoid/parasphenoid, with its postero-ventral margin forming the anterior border of both the otic capsule and the fenestra ovalis. The postero-dorsal surface of the prootic meets the supraoccipital dorsally, and ventrally overlaps the opisthotic. The antero-dorsal margin meets the parietal, but the suture is not clear. The lateral projection of the prootic extends for the anterior 1/3 of the paroccipital process.

## 2.2. Mandible (Figs 8, 9, 12, 13, 16)

The general construction of the mandible of *T. sulcognathus* is similar to that of other hyperodapedontine rhynchosaurs, its depth reaching more than 25% of the total length. The anterior (pre-symphyseal) tip forms the typical rhynchosaurid divergent tusk-like projections (Dilkes 1998; Hone & Benton 2008). The posterior portion is flat and broad. There is a large medial adductor fossa and an anteriorly developed meckelian canal.

**2.2.1. Dentary.** This crescent-shaped bone extends for more than half of the total length of the mandible, as in all Hyperodapedontinae, as well as in *Fodonyx spenceri* and *Rhynchosaurus articeps* (Benton 1990). Its anterior portion has an upwards and slightly lateral curvature that occludes medially with the premaxilla. This portion is devoid of any tooth remnant in UFRGS-PV-0232T and PV-0298T, but tooth rows in cross-section are visible in UFRGS-PV-0290T until near the anterior tip of the bone.

The dorsal surface of the dentary bears two well-developed, toothed, cutting blades and a medial projecting border. Both blades are more developed in the posterior third of the bone, becoming less conspicuous anteriorly, and unexpressed in its anterior third. In UFRGS-PV-0232T, these blades converge anteriorly, but in the other two specimens they extend almost in parallel for their entire length. Additionally, in UFRGS-PV-0290T, the blades are more anteriorly extended, and can be recognised near the tusk-like anterior process. The lateral blade is always more developed than the medial. In addition, there is a toothed prominent border medial to the medial blade, which extends to the anterior portion of the dentary as a restricted shelf.

The ventral portion of the dentary is composed of two descending laminae, medial and lateral to the meckelian canal. The lateral lamina is more ventrally extended and fits into a cleft on the dorso-lateral surface of splenial, as in *H. sanjuanensis*, *H. huxleyi* and *H. huenei* (Chatterjee 1974; Langer & Schultz 2000a; MACN-1885). The medial lamina is overlapped

ventrally by the splenial and posteriorly by the coronoid. The right mandible of UFRGS-PV-0298T lacks most of the dorsal portion of the medial ascending lamina of the splenial. This reveals the prearticular overlapping the dentary postero-ventrally under the splenial, as in *H. gordonii* (Benton 1983).

Both descending laminae have a shallow and elongated groove in their external surfaces. The medial groove is ventral to the medial-most tooth row, and seemingly accommodated the tongue (Chatterjee 1974). The lateral groove is more dorso-ventrally developed. Near its dorsal edge, a series of mental foramina of different sizes are visible, representing the lateral openings of the internal mandibular artery, external mandibular artery, and mandibular vein (Benton 1983). Near its antero-ventral margin, the dentary bears two large foramina, representing the external openings of the internal mandibular artery (Benton 1983).

**2.2.2. Splenial.** The splenial is composed of a thick ventral body and a medial ascending lamina that covers the dentary laterally. The anterior articulation to the dentary has a distinct V-shaped indentation, as in *H. gordonii* and *H. huxleyi* (Chatterjee 1974; Benton 1983). Below this, the splenial articulates to its opposite along its entire antero-medial margin, forming the complete mandibular symphysis, as in all Rhynchosauridae (Dilkes 1998; Hone & Benton 2008). In lateral view of the holotypic mandible (Fig. 9a), the splenial articulates to the dentary near the mandibular ventral edge. This is posteriorly continuous with the angular articulation, which is not laterally visible in UFRGS-PV-0298T. In medial view (Fig. 9b), the anterior portion of the splenial bears a clear anterior meckelian foramen, and two processes are present posteriorly. The small dorsal process is continuous with the splenial dorsal margin, and overlaps the prearticular anteriorly and the coronoid ventrally. The longer ventral process extends posteriorly, overlapping the prearticular in an oblique angle to the mandible ventral edge. At mid-length along that articulation, the well-developed elliptical posterior meckelian foramen is seen.

**2.2.3. Coronoid.** The coronoid is a complex bone that lies medially at the back of the mandibular tooth rows and forms the anterior border of the adductor fossa. Its ventral margin is overlapped by a dorsal process of the splenial, and interlocks with the prearticular more posteriorly, lateral to the splenial. The coronoid attaches antero-ventrally to the posterior edge of the dentary, and bears a small anterior process that conceals the posterior-most teeth of the medial dentary blade. Its lateral margin is overlapped by the medial surface of the dentary lateral blade. From that point forwards, the coronoid contacts the surangular medially and swings medially over the anterior margin of the adductor fossa.

**2.2.4. Angular.** The angular forms the posterior half of the mandibular floor and tapers anteriorly and posteriorly. In consequence, it forms the anterior part of the floor of both the adductor fossa and the meckelian canal. Its anterior portion contacts the splenial medially and expands dorsally, entering the lateral surface of the mandibular ramus. Its posterior process has little lateral expression and does not enter the medial surface of the mandible. Further, it overlaps the antero-ventral portions of the surangular laterally and the prearticular ventrally. In UFRGS-PV-0298T, a medial ascending lamina of the angular is seen lateral to the splenial. The posterior part of the angular is bound dorsally by the surangular and prearticular. These bones meet one another to form the floor of the adductor fossa, excluding the angular on which they rest. At its posterior-most extremity, the angular is wedged between the prearticular and articular, as compared to *H. gordonii* (Benton 1983), *H. huxleyi* (Chatterjee 1974) and *H. huenei* (Langer & Schultz 2000a), in which the angular does not contact the articular.

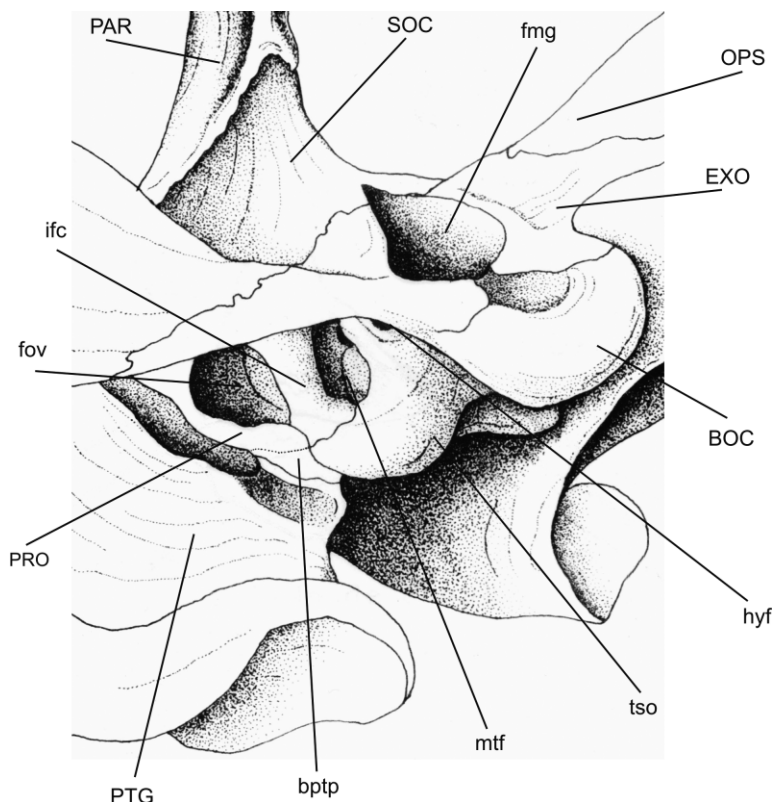


**Figure 7** *Teyumbaita sulcognathus*, holotype neurocranium in oblique view (UFRGS-PV-0232T), modified from Azevedo (1982). Abbreviations: BOC=basioccipital; bptp=basipterygoid process; EXO=exoccipital; fmg=fovea magna; fov=fenestra ovalis; hyf=hypoglossal foramen; ifc=interfenestral crest; mtf=metotic foramen; OPS=opisthotic; PAR=parietal; PTG=pterygoid; PRO=pro-otic; SOC=supraoccipital; tso=tubera sphenoccipitales.

**2.2.5. Surangular.** The surangular is composed of a deep and broad ventral portion and a lamina that extends antero-dorsally from its lateral margin, forming the posterior part of the meckelian channel and most of the lateral wall of the adductor fossa. The ventral portion forms the lateral base of the posterior mandibular ramus. Its ventro-lateral border is marked by a strong longitudinal keel, which extends further forwards, entering the angular, as in most *Hyperodapedon* (Benton 1983; Langer & Schultz 2000a). The surangular medial/postero-dorsal expansion borders the entire anterior/antero-lateral margins of the articular. This differs from the arrangement in *H. gordonii* and *H. huenei*, in which the surangular borders only the antero-lateral margin of that bone (Benton 1983; Langer & Schultz 2000a). As a consequence, the posterior border of the adductor fossa of *T. sulcognathus* is entirely formed by the surangular. The lateral ascending lamina also forms the lateral border of the adductor fossa and contacts the coronoid antero-dorsally. The surangular has a clear posterior supra-angular foramen on the posterior part of its lateral surface, as seen in various *Hyperodapedon* specimens (Chatterjee 1974; Benton 1983; Langer & Schultz 2000a; UFRGS-PV-0262T, UFRGS-PV-0408T, MCNSJ-574). Additionally, it bears the anterior supra-angular foramen, also present in *H. gordonii* (Benton 1983), and especially visible on the right mandibular of UFRGS-PV-0298T. As in *H. huxleyi* and *H. huenei* (Chatterjee 1974; Langer & Schultz 2000a), the surangular does not take part in the retroarticular process, except for its lateral support.

On the right mandible of UFRGS-PV-0298T (Figs 12–13), a well-developed aperture is seen on the lateral surface of the surangular, close to the angular articulation. This is circular, except for its antero-ventral margin, which seems to be broken. The aperture edge is smooth, suggesting an *in vivo* injury rather

than a result of scavenger action or a break after fossilisation. The opening is interpreted as pathological in origin, based on the partial left surangular of the same specimen that obviously lacks a similar opening (Fig. 13). Furthermore, since Dilkes (1998) reinterpreted Broom's early reports (Broom 1906) of a mandibular fenestra in *Mesosuchus*, no other rhynchosaur is known to possess this trait.

**2.2.6. Prearticular.** The prearticular forms the medial border of the adductor fossa and the postero-medial wall of the meckelian canal. The prearticular-articular articulation extends posteriorly and lies tangential to the ventral posterior border of the mandible, reaching its posterior-most tip. From this margin, the prearticular extends laterally, overlapping the angular posterior-most region. In the holotype, the posterior meckelian foramen pierces the prearticular, and its medial border is formed by the splenial. However, in UFRGS-PV-0298T, which lacks the splenial, the posterior meckelian foramen pierces only the prearticular.

**2.2.7. Articular.** The articular is a flat and broad element that forms the glenoid fossa. It lies dorsal to the posterior portions of the surangular laterally, and to the prearticular medially. The glenoid fossa is shallow, transversely elongate, more expanded laterally on the median portion, and with the same deepness through. This differs from *H. gordonii* and *H. huenei* (Benton 1983; Langer & Schultz 2000a), the glenoids of which have deeper medial and lateral regions. In addition, there are no well-developed ridges anterior and posterior to the glenoid fossa, as seen in some *Hyperodapedon* (Chatterjee 1974; Benton 1983; Langer and Schultz 2000a; UFRGS-PV-0408T, MCP-1693). The glenoid fossa is bordered by the surangular and prearticular laterally, and only by the former anteriorly. The posterior margin of the glenoid is bordered by a deep transverse groove, which is more developed medially.

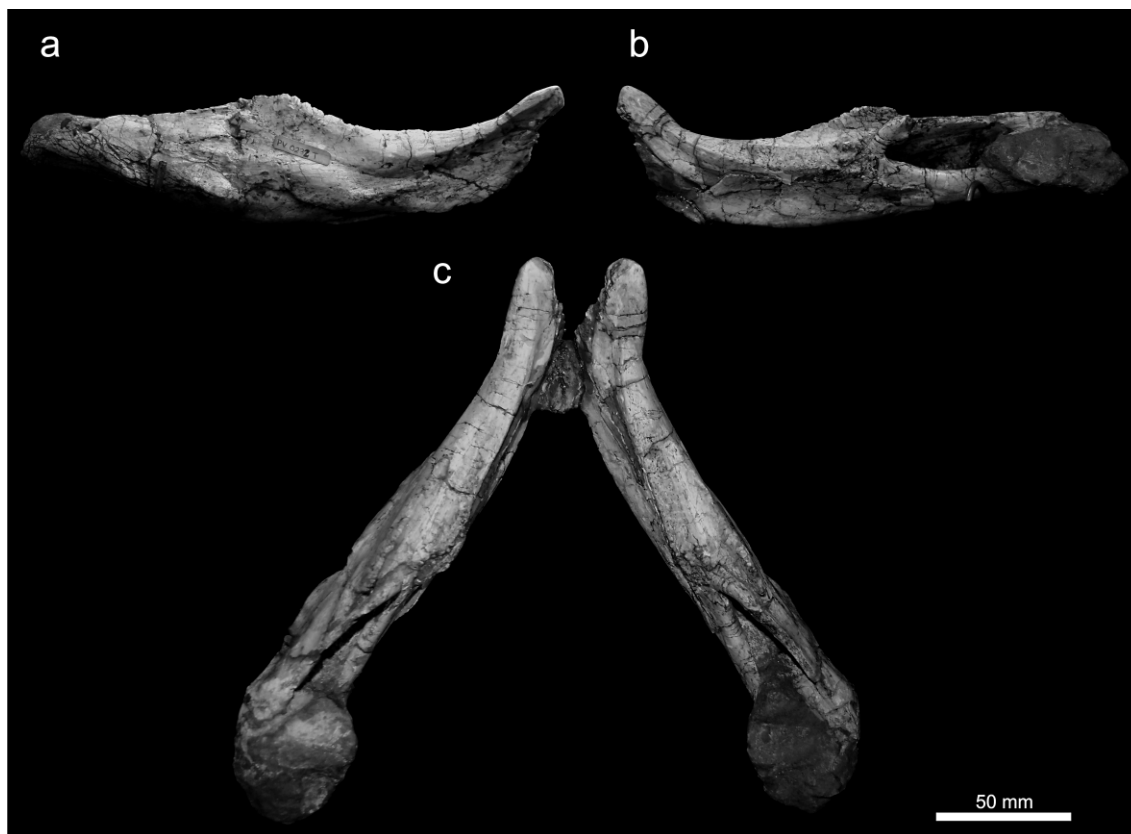


**Figure 8** *Teyumbaita sulcognathus*, holotype mandible (UFRGS-PV-0232T): (a) right ramus in lateral view; (b) right ramus in medial view; (c) mandible in occlusal view.

This forms a strong posteriorly expanded cavity, as seen in *H. gordonii*, *H. huxleyi* and *H. huenei* (Benton 1983; Langer & Schultz 2000a). Posterior to the cavity, the articular forms the retroarticular process, which is latero-ventrally covered by the surangular and medio-ventrally by the prearticular. In the holotype, it forms a low projection posterior to the glenoid fossa, with no upturned tip. On the other hand, UFRGS-PV-0298T possesses a well developed upturned retroarticular process, which is slightly anteriorly directed and bears a protuberance on its medial-most surface.

### 2.3. Dentition

*T. sulcognathus* has the typical general dental morphology of middle Late Triassic rhynchosaurs: an edentulous beak-like premaxilla and a blade and groove jaw apparatus, with dentary blades fitting precisely in the maxillary grooves. Teeth are present on the ventral and lingual regions of the maxilla, as well as on the top of blades and on the medial side of the dentary.

**2.3.1. Maxillary dentition.** For the maxillary dentition, following previous authors (Chatterjee 1969, 1980; Benton 1983, 1984b, 1990; Dilkes 1995; Langer & Schultz 2000a, b; Langer *et al.* 2000a, b; Nesbitt & Whatley 2004; Whatley 2005), the present authors assume homology between the lateral groove seen in the rhynchosaurs that bear two maxillary grooves, including *T. sulcognathus*, and the single maxillary groove of the other Hyperodapedontinae. Additionally, Chatterjee's (1974) categorisation of tooth rows is used in the maxilla. Accordingly, lateral rows to the main groove are labelled as L1, L2, etc, and those medial to the main groove as M1, M2, etc.

The maxillary dentition of *T. sulcognathus* is composed of three distinct tooth-bearing areas, which are separated posteriorly by two well-developed grooves that become confluent in

the anterior third of the bone. The lateral groove is deeper than the medial, and both are deeper posteriorly. The medial groove is narrower posteriorly and becomes wider anteriorly. The anterior confluence of the grooves, their anterior shallowing, and the increase in width of the medial groove are probably related to wear during previous ontogenetic stages, given that the grooves bear sectioned teeth, and obvious wear facets. Yet, on the posterior-most part of the maxilla, the grooves have no sign of wear, indicating that they are inherent features and not simply the result of wear, as already demonstrated by Benton (1984b) for rhynchosaurs in general.

As in other mid Late Triassic rhynchosaurs (Sill 1970; Chatterjee 1974; Benton 1983, 1984b; Azevedo 1984; Langer & Schultz 2000a; Langer *et al.* 2000a), there are two different kinds of tooth in the maxilla: the 'pyramidal' type and the conical type. In the three better-preserved specimens of *T. sulcognathus*, pyramidal teeth are more obviously seen on M1. This pattern differs from that of other Hyperodapedontinae, where pyramidal teeth are consistently on L1 (Sill 1970; Chatterjee 1974; Benton 1983, 1984b; Azevedo 1984; Langer & Schultz 2000a; Langer *et al.* 2000a). In fact, the differences between both tooth morphologies are not as clear-cut as in other members of that group (e.g., BSPHG-18.4, BSPHG-19.4, I.S.I.R. 17, MAL 1996 2, MCNSJ-588, MCP-1693). The pyramidal teeth are only slightly antero-posteriorly compressed compared to the conical ones, which have a circular to elliptical cross-section.

In the posterior part of the maxilla, the medial tooth-bearing area is wider than the lateral. This condition is shared by most late Middle Triassic rhynchosaurs (except *Ammorhynchus navajoi*) and *Hyperodapedon huenei*, and is usually considered plesiomorphic among rhynchosaurids (Benton 1990; Langer & Schultz 2000a; Langer *et al.* 2000a; Hone & Benton 2008). The lateral tooth-bearing area is crest-shaped,

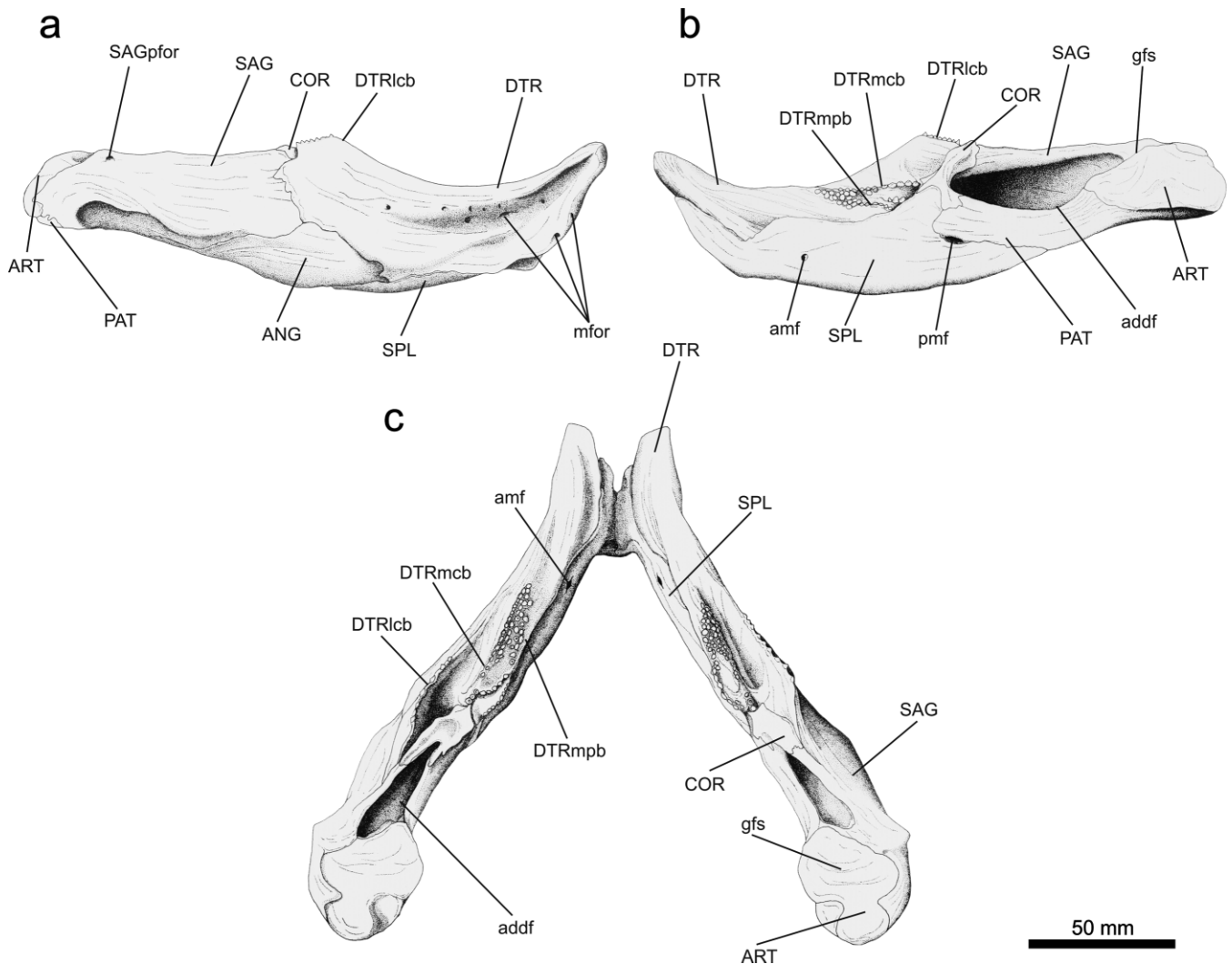


**Figure 9** *Teyumbaita sulcognathus*, holotype mandible (UFRGS-PV-0232T) modified from Azevedo (1982): (a) right ramus in lateral view; (b) right ramus in medial view; (c) mandible in occlusal view. Abbreviations: amf=anterior meckelian foramen; addf=medial adductor fossa; ANG=angular; ART=articular; COR=coronoid; DTR=dentary; DTRlcb=lateral cutting blade of dentary; DTRmcb=medial cutting blade of dentary; DTRmpb=medial projecting border of dentary; gfs=glenoid fossa; mfor=mental foramen; PAT=prearticular; pmf=posterior meckelian foramen; SAG=surangular; SAGpfor=posterior supra-angular foramen; SPL=splénial.

resembling that of Middle Triassic rhynchosaurs (Langer *et al.* 2000a), and composed of three longitudinal tooth rows. L1 is composed of packed teeth, extending from the posterior-most part of the maxilla to reach its anterior portion. L2 arises more anterior on the maxilla, also reaches its anterior portion, but is composed of more widely spaced teeth. L3 is somewhat different in the three better-known specimens. In the holotype, it is composed of five teeth, seen only on the median portion of the right maxilla. In UFRGS-PV-0298T, this row has the same extent as L2. In UFRGS-PV-0290T, it is represented by only two teeth, as seen on the preserved part of the lateral tooth-bearing area of the left maxilla.

The central tooth-bearing area (between the grooves) shows a single longitudinal tooth row (M1) in the holotype and UFRGS-PV-0298T. The tooth crowns are visible only on the posterior region, probably representing a nonfunctional area for mastication. In the holotype, worn teeth are not visible, possibly due to preservation, but in UFRGS-PV-0298T they extend as far as the area where the grooves become confluent. In UFRGS-PV-0290T, the central tooth-bearing area also bears a M1 with crowns in its posterior region, plus worn teeth extending to the confluence of the grooves. Yet, midway along the row, additional teeth are, especially visible in the right maxilla.

The medial tooth-bearing area is more complex in *T. sulcognathus*, varying among specimens in the number of tooth rows and the morphology of the medial edge. Teeth are mostly worn flat in that area and crowns are only present on its posterior half. The holotype has a crest-shaped medial tooth-bearing area, similar to the lateral one, which finishes in an abrupt medial edge. On the left maxilla a single longitudinal row is seen on the top of the crest, starting in its posterior-most region and extending anteriorly. Additionally, three teeth are present lateral to the row in its posterior-most region, but they do not form a clear row. On the right maxilla, the same longitudinal row is present, lateral to which a single complete tooth crown is seen, along with four worn down teeth. On the lingual side of each holotypic maxilla, there is a single lingual tooth, which does not occlude with the dentary.

In contrast, UFRGS-PV-0298T and UFRGS-PV-0290T have a cushion-shaped medial portion of the maxilla that does not finish in an abrupt medial edge. Accordingly, the more medially placed teeth are somewhat continuous with the lingual teeth, as also seen in *Hyperodapedon gordonii* and *H. huenei* (Benton 1983; Langer & Schultz 2000a). In addition, a greater number of tooth crowns are unworn, but the precise number of rows is difficult to determine. The rows seem to be

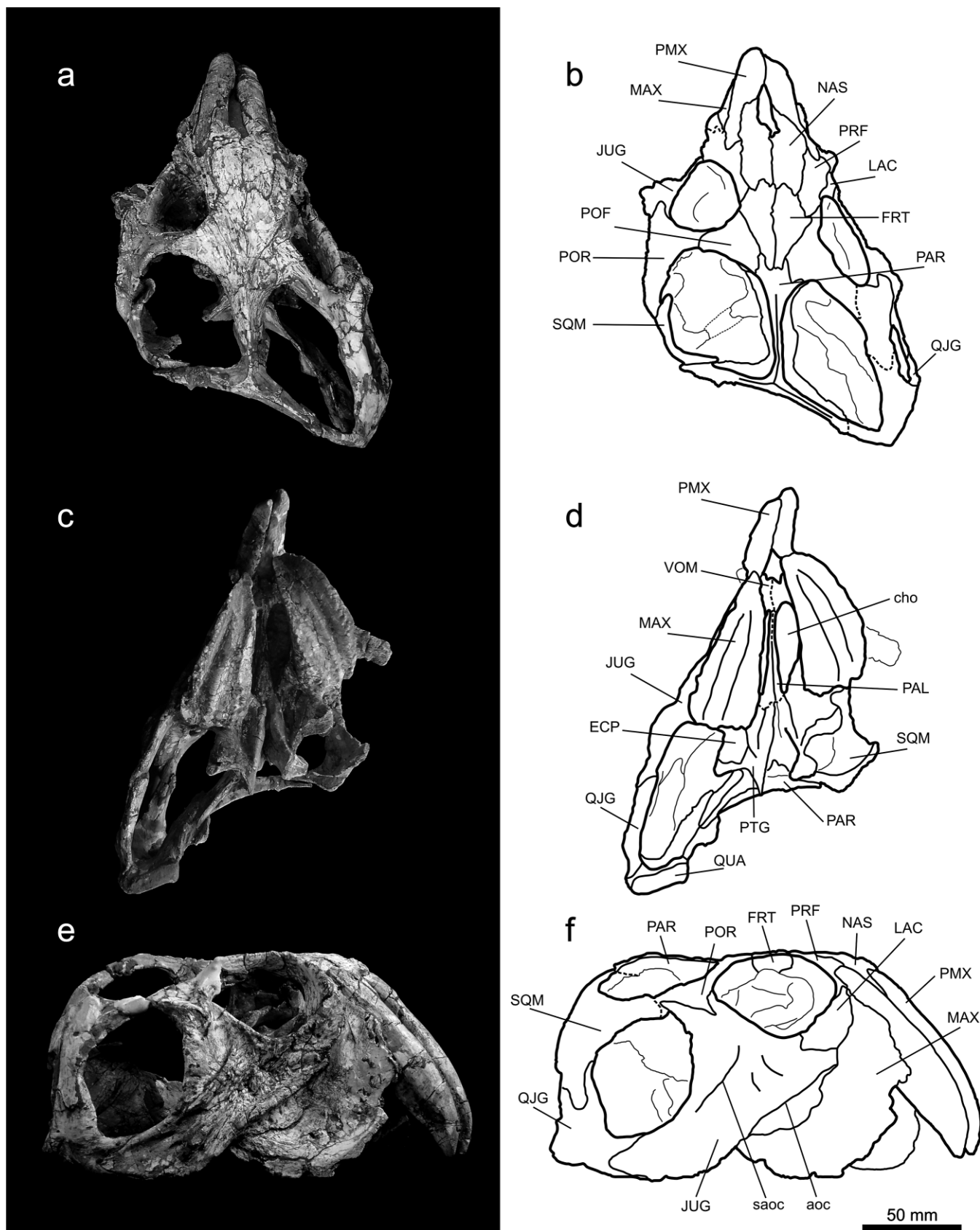


**Figure 10** *Teyumbaita sulcognathus*, referred skull (UFRGS-PV-0298T): (a) dorsal view; (b) outline drawing of dorsal view; (c) ventral view; (d) outline drawing of ventral view; (e) right lateral view; (f) outline drawing of right lateral view. Dashed lines represent inferred sutures and reconstructed parts. Abbreviations: aoc=*anguli oris* crest; cho=choana; ECP=ectopterygoid; FRT=frontal; JUG=jugal; LAC=lacral; MAX=maxilla; NAS=nasal; PAL=palatine; PAR=parietal; PMX=premaxilla; POF=postfrontal; POR=postorbital; PRF=prefrontal; PTG=pterygoid; QJG=quadratojugal; QUA=quadrate; saoc=secondary *anguli oris* crest; SQU=squamosal; VOM=vomer.

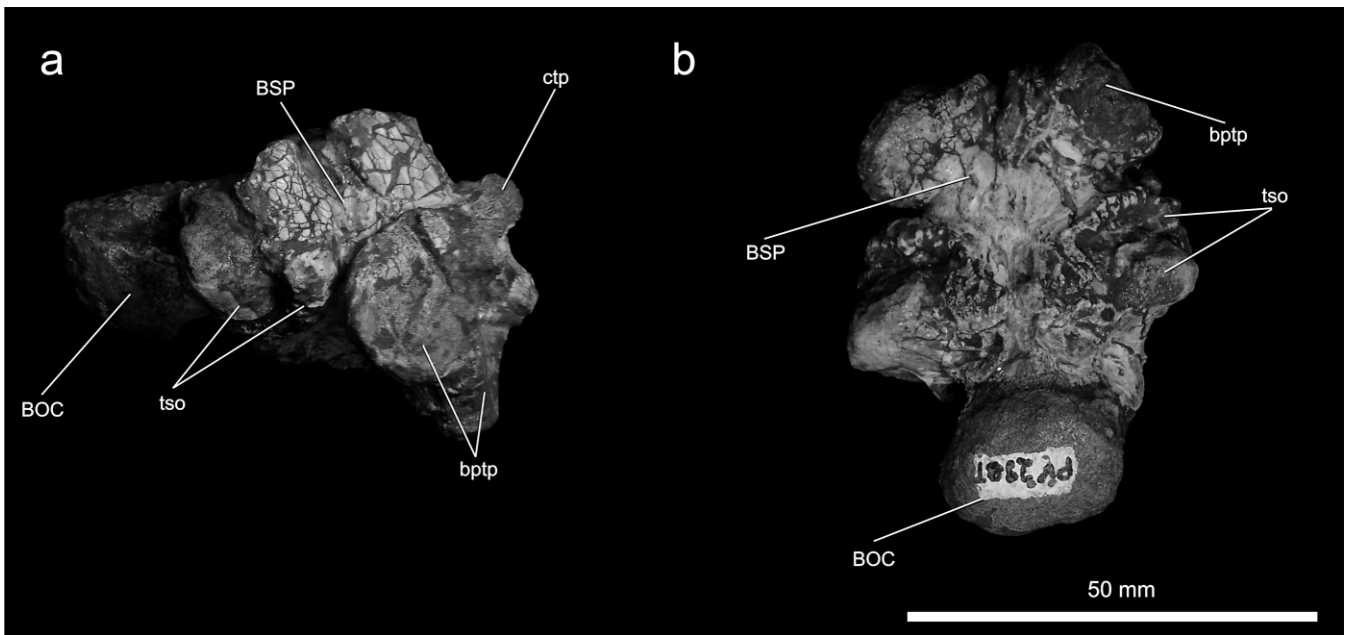


**Figure 11** *Teyumbaita sulcognathus*, referred neurocranium (UFRGS-PV-0298T): (a) right lateral view; (b) ventral view. Abbreviations: BOC=basioccipital; bptp=basipterygoid process; BSP=basisphenoid/parasphenoid; ctp=cultriform process; tso=tubera sphenooccipitales.

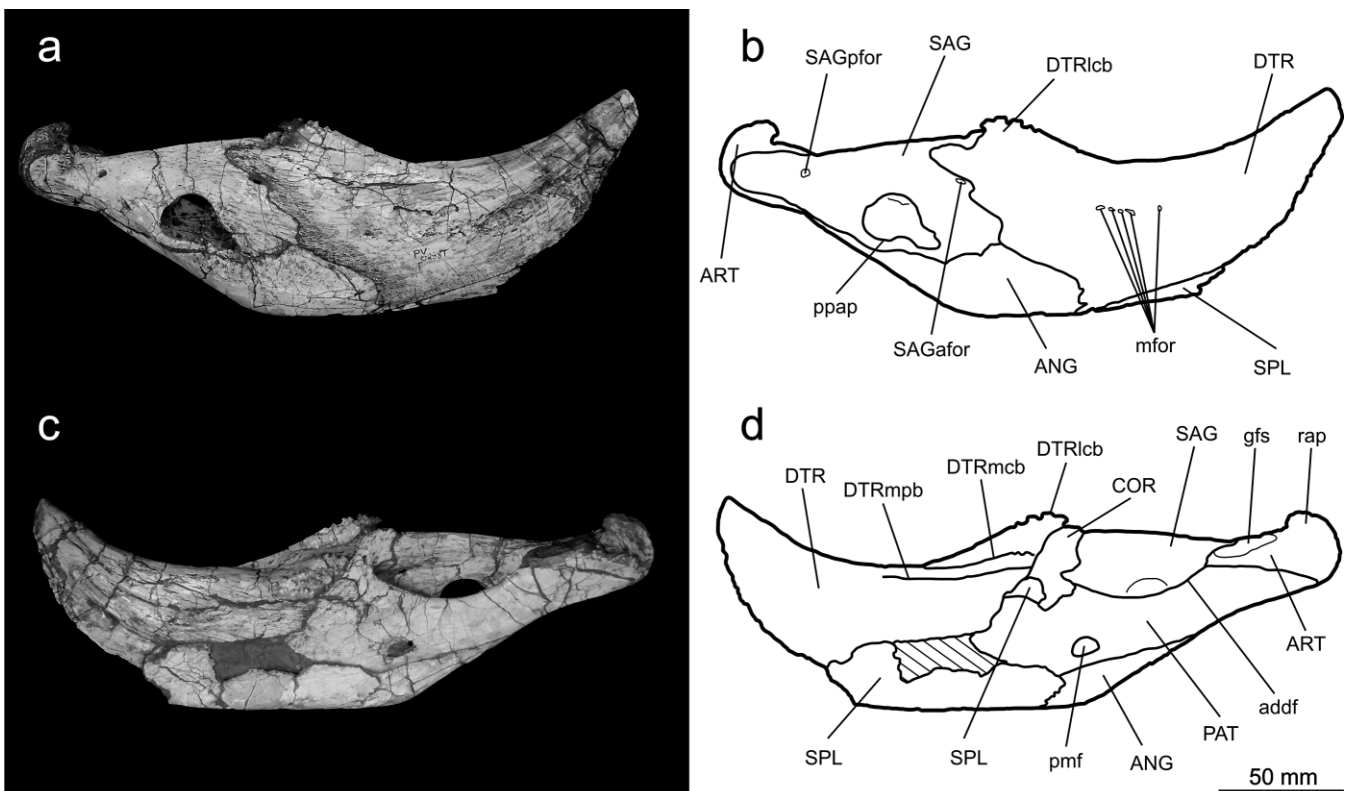


**Figure 12** *Teyumbaita sulcognathus*, referred right mandibular ramus (UFRGS-PV-0298T): (a) lateral view; (b) outline drawing of lateral view; (c) medial view; (d) outline drawing of medial view; dashed area represents a damaged portion of the mandible. Abbreviations: addf=medial adductor fossa; ANG=angular; ART=articular; COR=coronoid; DTR=dentary; DTRlcb=lateral cutting blade of dentary; DTRmcb=medial cutting blade of dentary; DTRmpb=medial projecting border of dentary; gfs=glenoid fossa; mfor=mental foramen; PAT=prearticular; pmf=posterior meckelian foramen; ppap=paleopathological aperture; rap=retroarticular process; SPL=splenic; SAG=surangular; SAGafor=anterior supra-angular foramen; SAGpfor=posterior supra-angular foramen.

arranged longitudinally rather than transversely (*contra* Chatterjee 1974; Langer & Schultz 2000a), and at least three rows of conical teeth seem to be present. Teeth forming the three rows are mainly visible in cross-section along the posterior two thirds of the maxilla. In UFRGS-PV-0298T, an

extra, widely spaced row is present medial to the other three. These could be considered lingual teeth, because they are not worn and placed on the medial maxillary edge. Yet, UFRGS-PV-0290T also bears this extra row, and its anterior teeth are worn, suggesting occlusion during at least some period of the

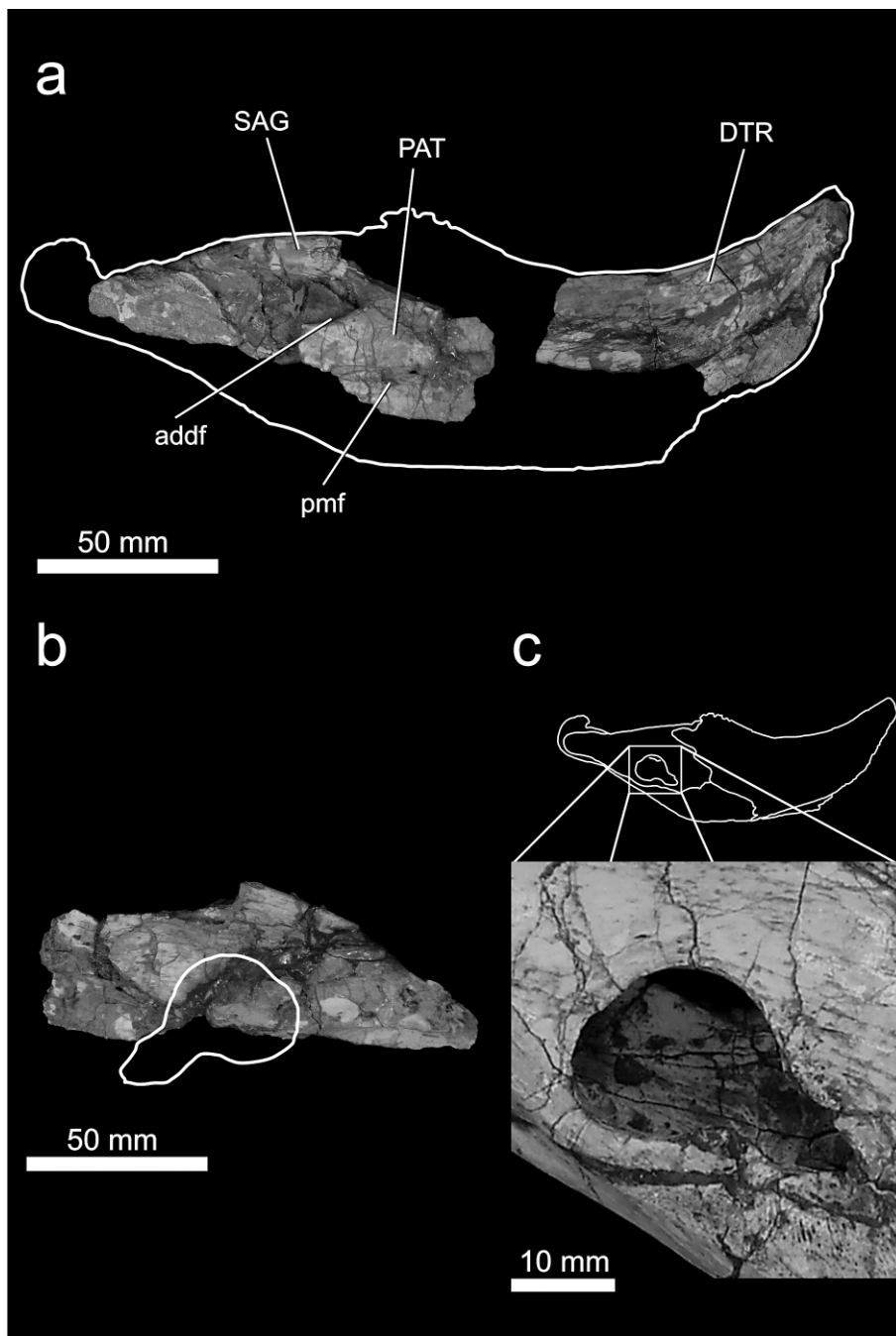


**Figure 13** *Teyumbaita sulcognathus*, referred left and right mandibular rami (UFRGS-PV-0298T): (a) outline of left ramus showing the preserved parts in medial view; (b) left surangular in lateral view, with outline of the palaeopathological aperture of the right side in the inferred corresponding position; (c) outline of the right ramus, highlighting the palaeopathological aperture. Abbreviations: addf=medial adductor fossa; DTR=dentary; PAT=prearticular; pmf=posterior meckelian foramen; SAG=surangular.

animal's life. Accordingly, these are not considered strict lingual teeth, which are represented only by a single element, as also seen in the holotype, and interpreted as a synapomorphy of *T. sulcognathus*.

**2.3.2. Mandibular dentition.** This description follows Benton's (1984b) topological differentiation of buccal and lingual teeth, and the nomenclature for lingual teeth proposed by Langer & Schultz (2000a). The heavily packed buccal teeth of *T. sulcognathus* are small, antero-posteriorly compressed, and distributed along a well-defined longitudinal row on top of the lateral dentary blade, as seen in other Hyperodapedontinae. These morphologically differentiated teeth are equivalent to those borne on the single dentary blade of other Hyperodapedontinae. Tooth crowns are integral only on the posterior-

most portion of the blade, which is mainly composed of worn down teeth. Yet, the anterior portion of the holotypic dentary is totally devoid of teeth, and not even cross-sections are seen.

The lingual teeth of *T. sulcognathus* are conical, larger than the buccal, close to one another, and arranged in a complex pattern. A rather obvious tooth row is seen on top of a medial crest that forms a cutting blade in the posterior part of the dentary of UFRGS-PV-0232T and PV-0298T. In the anterior portion of the bone, this row is indistinct in UFRGS-PV-0232T, but can be traced as far as its anterior portion in UFRGS-PV-0298T. In UFRGS-PV-0290T this row could be interpreted as that topping the much less expressed medial crest, seen in the preserved anterior portion of the dentary. Following the argumentation of Langer & Schultz (2000a) and

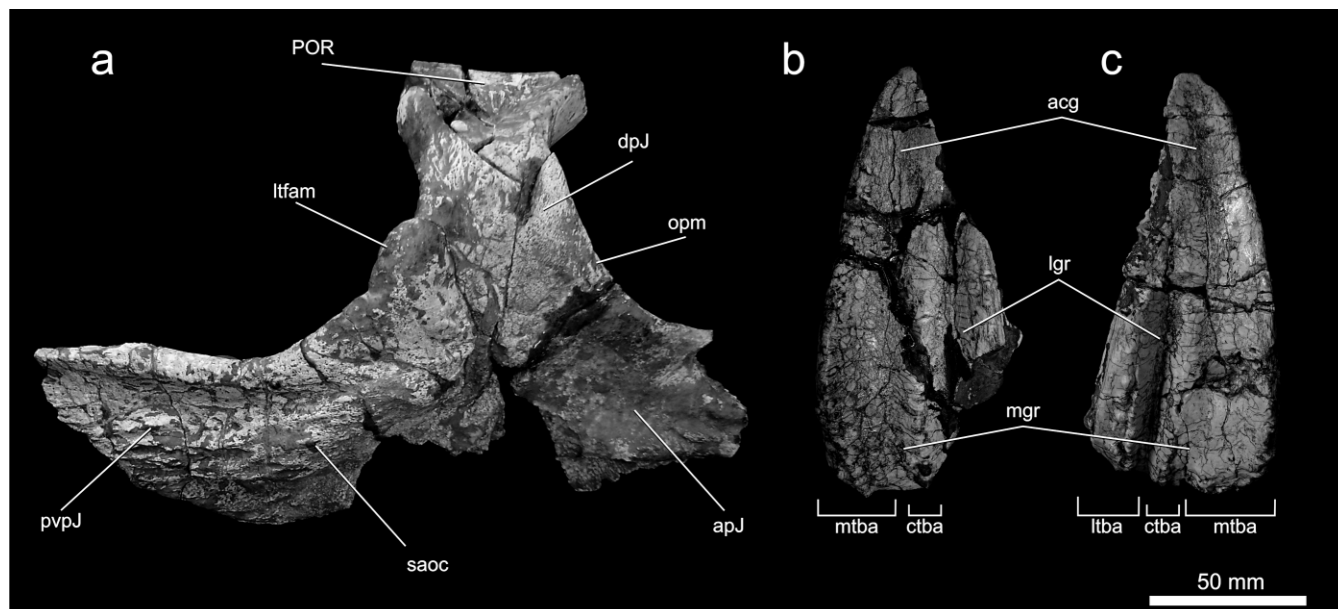


**Figure 14** *Teyumbaita sulcognathus*, referred skull parts (UFRGS-PV-0290T): (a) lateral view of the right jugal; (b) left maxilla in occlusal view; (c) right maxilla in occlusal view. Abbreviations: acg=anterior confluent grooves; apJ=anterior process of the jugal; ctba=central tooth-bearing area; dpJ=dorsal process of the jugal; ltfam=anterior lateral groove; ltba=lateral tooth-bearing area; mgr=medial groove; mtba=medial tooth-bearing area; opm=orbital posterior margin; POR=postorbital; pvpj=postero-ventral process of the jugal; saoc=secondary *anguli oris* crest.

Langer *et al.* (2000a), this medial row in *T. sulcognathus* is interpreted as homologous to that resting on top of the medial ridge in *Rhynchosaurus articeps*, *Stenaulorhynchus stockleyi*, *Fodonyx spenceri* and the ‘Rincossauro de Mariante’, and to the lingual teeth of *Isalorhynchus genovefae*, *H. gordonii*, *H. huxleyi*, *H. mariensis* and *H. huenei*.

Medial to the medial cutting blade there are numerous primary lingual teeth (*sensu* Langer & Schultz 2000a), interpreted as homologous to the medially displaced teeth of *Rhynchosaurus articeps*, *Fodonyx spenceri*, *Stenaulorhynchus stockleyi* and the ‘Rincossauro de Mariante’. These teeth are located on a projecting border that extends along the length of the dentary. More posteriorly, the teeth seem to be arranged in diagonal rows of three or four, but the rows are blurred anteriorly, and the teeth seem to be oriented longitudinally. This configuration of teeth on a projecting border, forming a tooth battery that extends along the whole medial length of the dentary, is similar to that seen in *Stenaulorhynchus stockleyi*, *Fodonyx spenceri* and the ‘Rincossauro de Mariante’.

### 3. Discussion

As long suspected, the results obtained by the present authors support the assignment of the taxon originally described by Azevedo & Schultz (1987) as *Scaphonyx sulcognathus* to a new genus herein named *Teyumbaita*. Its uniqueness is supported by several cranial autapomorphies (see diagnosis above) that distinguish *Teyumbaita* from other rhynchosaurs.

Partially due to their abundance, most accounts of rhynchosaur evolution and taxonomy are based on the study of the tooth-bearing bones (Chatterjee 1969, 1980; Langer & Schultz 2000a; Langer *et al.* 2000a; Hone & Benton 2008). This is particularly the case among Hyperodapedontinae, the skeleton of which is remarkably conservative (Benton 1983; Langer & Schultz 2000a; Langer *et al.* 2000b; Nesbitt & Whatley 2004). One of the dental traits most often discussed in the context of rhynchosaur evolution is the presence/absence of a subsidiary

medial groove on the maxillary tooth plate, when the presence of such a groove is traditionally considered the plesiomorphic condition (Langer 1996; Langer & Schultz 2000a; Langer *et al.* 2000a; Hone & Benton 2008). Based on that premise, *Teyumbaita sulcognathus* would fall basal to the other Hyperodapedontinae, including *H. huenei* and more derived *Hyperodapedon* species (Langer & Schultz 2000a, b; Langer *et al.* 2000a, b; Hone & Benton 2008). Yet, Nesbitt & Whatley (2004), based on the study of the single grooved maxilla of the Middle Triassic rhynchosaur *Ammorhynchus navajoi*, challenged this traditional interpretation, suggesting the possibility that the subsidiary groove represents an apomorphic trait. In this alternative scenario, *Teyumbaita sulcognathus* would represent a derived form of Hyperodapedontinae, a hypothesis corroborated by its higher stratigraphic position.

The higher stratigraphic placement of *T. sulcognathus* relative to *Hyperodapedon sensu* Langer *et al.* (2000a, b) is seen in all sites that yield specimens of both taxa (Fig. 1). Indeed, no *Hyperodapedon*-related form has ever been positively identified above or at the same level as *T. sulcognathus*, while the proposed correlation of sites that separately bear these taxa is inconclusive. Based on the correspondence between the *Hyperodapedon*-rich and *Jachaleria*-bearing faunas of the Rosário do Sul and Água de la Peña groups, and the inferred intermediate position of strata bearing *T. sulcognathus*, Langer *et al.* (2007) proposed their correlation to the upper levels of the Ischigualasto Formation, Argentina, the top of which has recently provided a  $^{40}\text{Ar}/^{39}\text{Ar}$  age of  $217.0 \pm 1.7$  Ma (Currie *et al.* 2008). This corresponds to the latest Carnian in the scheme of Ogg (2004), but recent work (Muttoni *et al.* 2001, 2004; Gallet *et al.* 2003; Kent *et al.* 2006; Walker & Geissman 2009) extended the Carnian–Norian boundary to about 228 Ma. Following these proposals, and the age recalculation of the lower third of the Ischigualasto Formation (Furin *et al.* 2006), only strata that rest above *Hyperodapedon*-rich deposits can be safely regarded as Norian, as is the case for those that yielded *T. sulcognathus*.

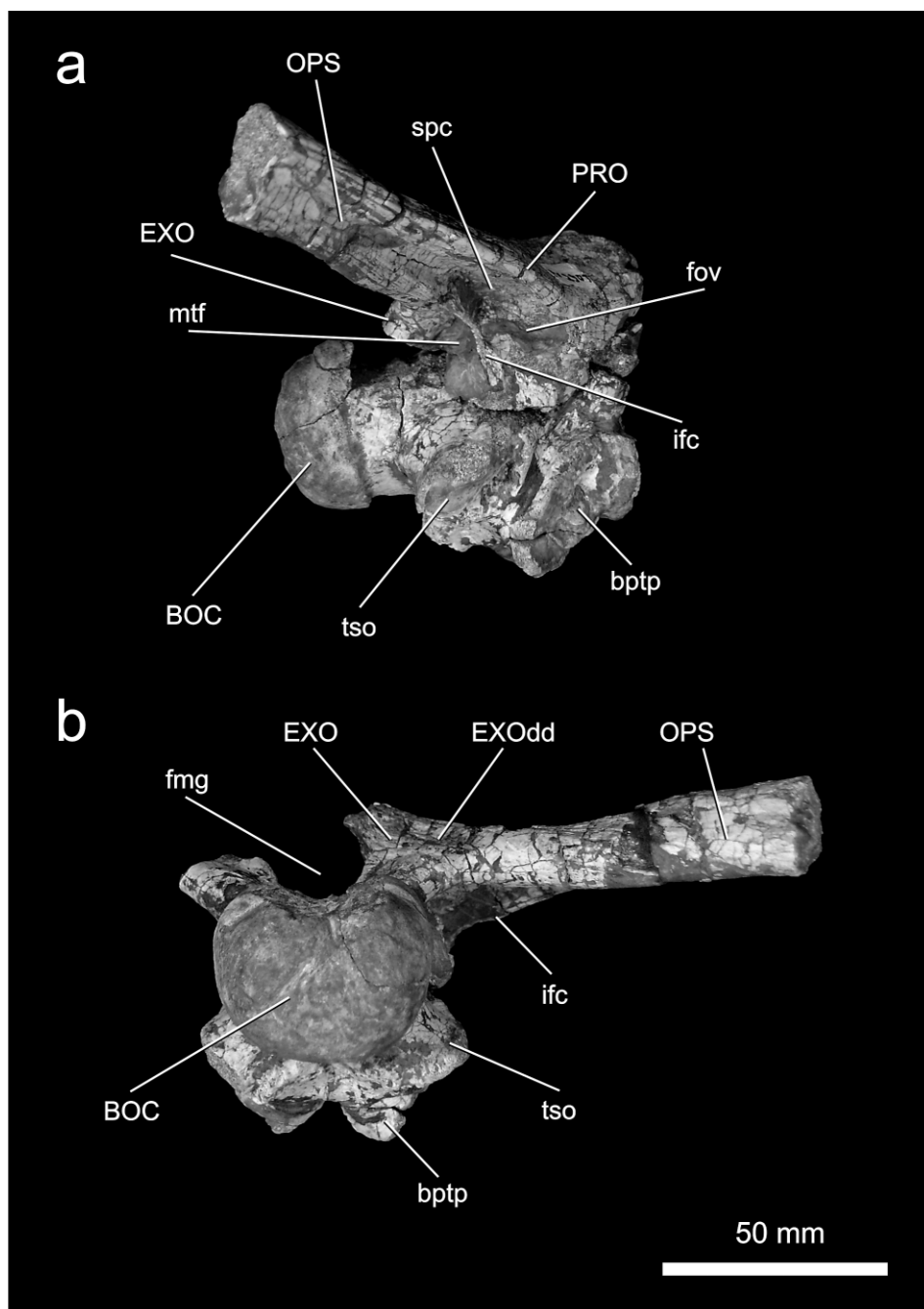


**Figure 15** *Teyumbaita sulcognathus*, referred neurocranium (UFRGS-PV-0290T): (a) right lateral view; (b) occipital view. Abbreviations: BOC=basioccipital; btp=basipterygoid process; EXO=exoccipital; EXOdd=distinct depression of the exoccipital; fmg=foramen magnum; fov=fenestra ovalis; ifc=interfenestralis crest; mtf=metotic foramen; OPS=opisthotic; PRO=pro-otic; spc=stapedial canal; tso=tubera sphenooccipitales.

### 3.1. Phylogenetic analysis

In order to investigate the phylogenetic position of *T. sulcognathus* among Rhynchosauria, parsimony analyses were performed based on new and on previously proposed characters (Benton 1988, 1990; Dilkes 1995, 1998; Langer & Schultz 2000a; Langer *et al.* 2000a; Whatley 2005; Hone & Benton 2008). Two outgroup and seven ingroup taxa were selected (see Appendix 1) and 59 informative characters (see Appendix 2) were defined. The data matrix (Appendix 3) was analysed using the software *TNT version 1.1* (Goloboff *et al.* 2008) under the implicit enumeration algorithm, constraining *Mesosuchus* as the basal most taxon and *Howesia* as the sister-group of the ingroup (Rhynchosauridae *sensu* Dilkes 1998). A single most parsimonious tree (94 steps) was obtained (Fig. 17), in

which *Rhynchosaurus* was placed as the basal most Rhynchosauridae, as in Dilkes (1995, 1998), Langer (1996), Langer & Schultz (2000b), Langer *et al.* (2000b) and Whatley (2005). *Stenaulorhynchus* and the 'Rincossauro de Mariante' formed a clade basal to *Fodonyx* and Hyperodapedontinae, as suggested by Langer & Schultz (2000b) *contra* Hone & Benton (2008). As proposed by Hone & Benton (2008), *Fodonyx* is the sister group of Hyperodapedontinae, which includes *Isalorhynchus* as its basal most taxon, as suggested by Whatley (2005); *contra* Langer *et al.* (2000b). The affinity of *Teyumbaita* to *Hyperodapedon* is supported by several apomorphic traits (see Appendix 2), e.g., postorbital ventral process entering on the dorsal margin of the jugal; basipterygoid process wider than long; more than one clear tooth row laterally to main

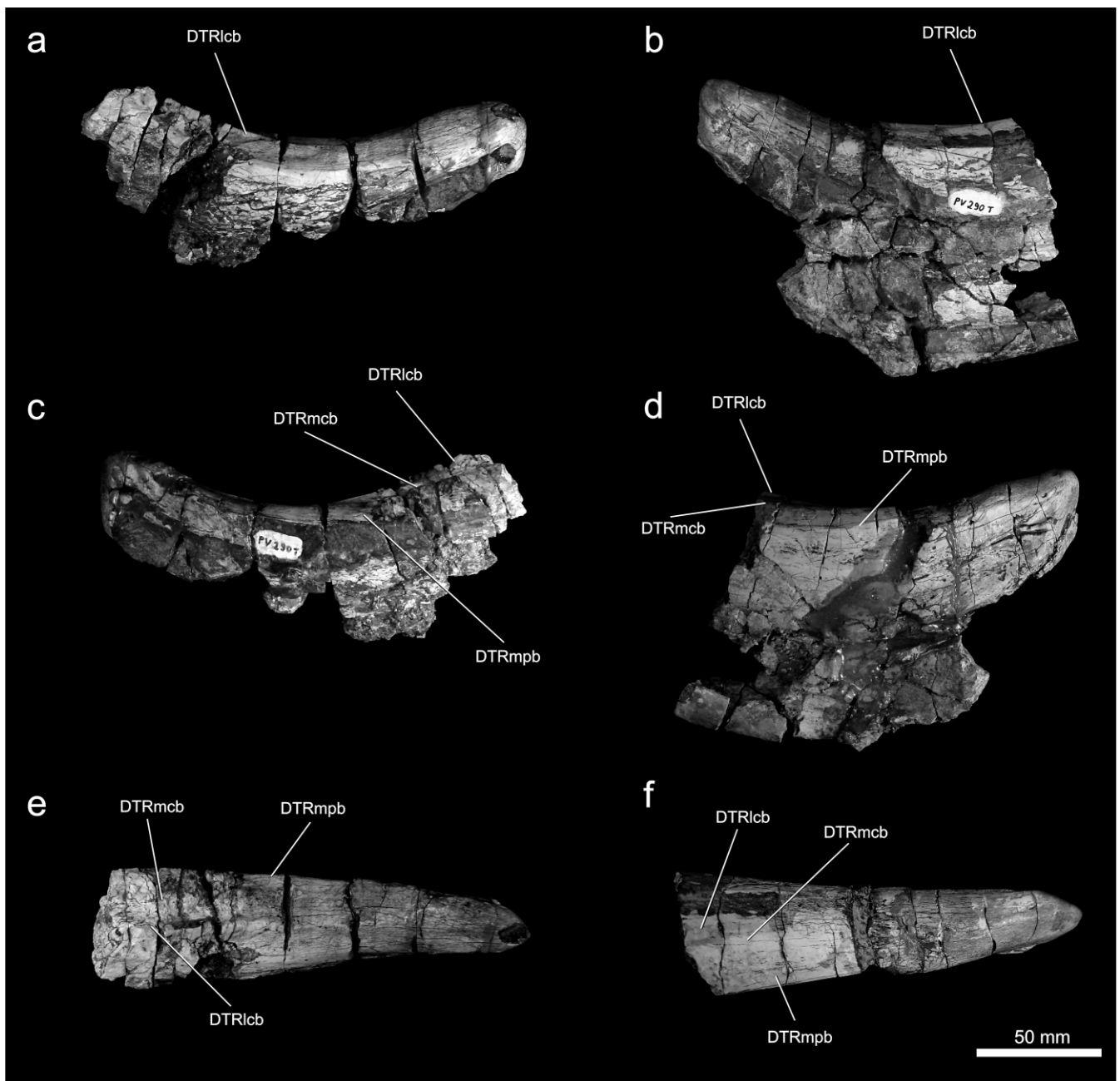


**Figure 16** *Teyumbaita sulcognathus*, referred mandible (UFRGS-PV-0290T): (a) right ramus in lateral view; (b) left ramus in lateral view; (c) right ramus in medial view; (d) left ramus in medial view; (e) right ramus in occlusal view; (f) left ramus in occlusal view. Abbreviations: DTRlcb=lateral cutting blade of dentary; DTRmcb=medial cutting blade of dentary; DTRmpb=medial projecting border of dentary.

maxillary groove; and crest-shaped epiphyses on cervical postzygapophyses.

#### 4. Acknowledgements

The authors are especially grateful to Sérgio Alex K. Azevedo for permission to use the previously unpublished data and figures of the holotype of *T. sulcognathus* from his MSc Thesis, and for helpful information on the provenance of this and other specimens. The authors also wish to thank M. Benton and J. C. Cisneros for the critical review of the manuscript, and A. M. Sá Teixeira for the skillful drawings of the holotypic skull. Financial support was provided by the Conselho Nacional de Desenvolvimento Científico e Tecnológico (CNPq) and by the Programa de Pós-Graduação em Biologia Com-

parada, Faculdade de Filosofia Ciências e Letras de Ribeirão Preto–USP.

#### 5. Appendices

##### 5.1. Appendix 1. Operational taxonomic units

Ingroup and outgroup operational taxonomic units used in the phylogenetic analysis.

Sources of data for coding are listed for each taxon (specimens studied firsthand and published descriptive accounts). *T. sulcognathus* was coded based on the three specimens described here.

##### Outgroup

*Mesosuchus* – *Mesosuchus browni* Watson, 1912 (SAM-5882, SAM-6536, SAM-7416, SAM 7701; Dilkes 1998).

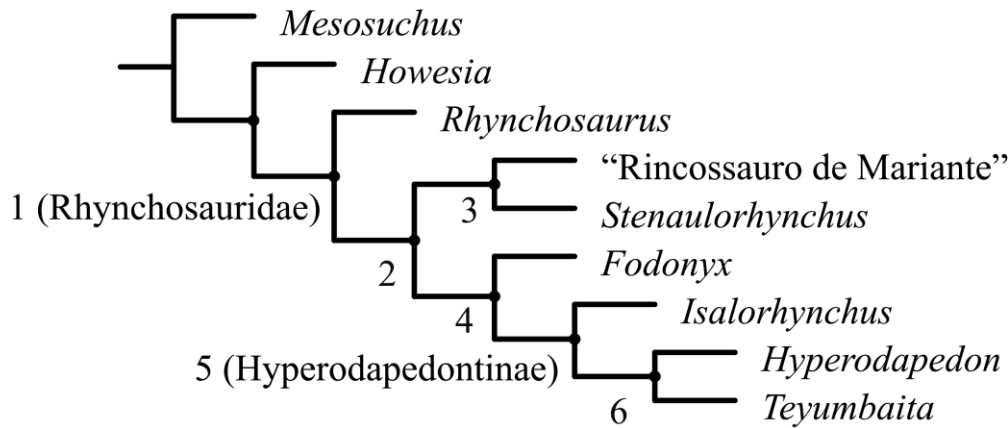


**Figure 17** Cladistic analyses of the relationships within Rhynchosauria. Single most parsimonious tree showing node numbers and names. Clade synapomorphies are given in Appendix 2 and complete data matrix in Appendix 3.

*Howesia* – *Howesia browni* Broom, 1906 (SAM-5884, SAM-5885, SAM-5886; Dilkes 1995).

### Ingroup

*Rhynchosaurus* – *R. articeps* Owen, 1842 and *R. brodiei* Benton, 1990 (SHRBM G-132/1982, BMNH R-1236, BMNH R-1237, BMNH R-8495; Benton 1990).

*Stenaulorhynchus* – *S. stockleyi* Haughton, 1932 (IGMPT-317 A/B; Huene 1938).

'Rincossauro de Mariante' – Taxon not formally described see Schultz & Azevedo (1990) (UFRGS-PV-0168T, UFRGS-PV-0315T).

*Fodonyx* – *F. spenceri* Benton, 1990 (BRSUG 27200, EX 79/1992; Hone & Benton 2008).

*Isalorhynchus* – *Isalorhynchus genovefae* Buffetaut, 1983 (Whatley 2005).

*Hyperodapedon* – *H. gordonii* Huxley, 1859; *H. huxleyi* Lydekker, 1885; *H. mariensis* Tupi Caldas, 1933; *H. sanjuanensis* Sill, 1970; *H. huenei* Langer & Schultz, 2000a (BMNH-R-699, BMNH-G281/1; FZB-PV-1867, MACN-18185, UFRGS-0132; Benton 1983; Chatterjee 1974; Sill 1970; Langer & Schultz 2000a).

### 5.2. Appendix 2. Character descriptions

The 59 characters used in the phylogenetic analyses are described below (along with the character-states). The character–taxon matrix is presented in Appendix 3. Characters, 36, 43 and 47 were treated as additive. Characters are either new or adapted from previously published analyses (acknowledged accordingly).

- Skull dimensions. Longer than broad (0); broader than long (1) (Benton 1984a, 1985, 1988, 1990; Dilkes 1995, 1998; Langer 1996; Langer & Schultz 2000a; Whatley 2005; Hone & Benton 2008).
- Skull height. Less than 50% of the midline length (0); more than 50% of the midline length (Hone & Benton 2008).
- Orbit orientation. Mostly lateral (0); mostly dorsal (1) (Langer & Schultz 2000a; Hone & Benton 2008).
- Orbital medial margin. Rounded (0); forming a marked angle (1).
- Jugal and maxillary heights below the orbit ventral margin. Maxilla higher (0); jugal higher (1) (Benton 1984a, 1985, 1988, 1990; Hone & Benton 2008).
- Jugal-lacrimal contact. Minimal (0); extensive contact of the jugal anterior process (1) (Whatley 2005).
- Jugal lateral surface. *Anguli oris* crest does not reach jugal anterior process (0); *anguli oris* crest reaches jugal anterior process (1) (Benton 1984a, 1988; Dilkes 1995, 1998; Langer & Schultz 2000a; Whatley 2005; Hone & Benton 2008).
- Jugal surface dorsal to *anguli oris* crest. Lacking a secondary crest (0); with a secondary *anguli oris* crest (1) (Langer & Schultz 2000a; Whatley 2005; Hone & Benton 2008).
- Lateral overlap of maxilla by jugal. Absent or minimally expanded (0); well developed (1) (Whatley 2005).
- Jugal subtemporal process. Height more than 50% of the length (0); height less than 50% of the length (1) (Dilkes 1995, 1998; Whatley 2005).
- Relative widths of postorbital bar and lower temporal fenestra. Less than 0.4 (0); more than 0.4 (1) (Langer & Schultz 2000a; Whatley 2005; Hone & Benton 2008).
- Dorso-medial surface of prefrontal near the orbital rim. Flat or slightly concave (0); deeply concave (1) (Whatley 2005).
- Procumbent lacrimal and prefrontal antero-lateral margin. Absent (0); present (1) (Whatley 2005).
- Dorsal groove on frontal. Deeper posteriorly (0); same depth throughout its length (1) (Dilkes 1995, 1998; Langer & Schultz 2000a; Whatley 2005; Hone & Benton 2008).
- Well marked V-shaped crest along frontal-postfrontal contact. Absent (0); present (1).
- Frontal and parietal midline lengths. Frontal longer (0); parietal longer (1) (Benton 1988, 1990; Dilkes 1995, 1998; Whatley 2005; Hone & Benton 2008).
- Postfrontal. Excluded from upper temporal fenestra border (0); forming the upper temporal fenestra border (1) (Dilkes 1998; Whatley 2005; Hone & Benton 2008).
- Postfrontal dorsal surface. Flat (0); markedly concave (1) (Dilkes 1995, 1998; Whatley 2005; Hone & Benton 2008).
- Postorbital antero-ventral process. Expanding ventral to the level of the orbital midpoint (0); expanding dorsally to orbital height midpoint (1) (Dilkes 1998; Whatley 2005; Hone & Benton 2008).
- Postorbital ventral process. Expands anterior to the jugal (0); fits dorsal to the jugal (1) (Whatley 2005).
- Postorbital–parietal suture. Visible in dorsal view (0); hidden in dorsal view (1) (Dilkes 1998; Whatley 2005).
- Parietal body. Not expanded laterally at midlength (0); expanded laterally at midlength (1).
- Parietal transverse process. Postero-laterally directed (0); laterally directed (1).
- Distal tip of parietal transverse process. Not anteriorly curved (0); anteriorly curved (1).
- Squamosal ventral process. Thinner than 50% of dorso-ventral length (0); broader than over 50% of dorso-ventral

- length (1) (Benton 1990; Langer & Schultz 2000a; Hone & Benton 2008).
26. Relative position of quadratojugal and squamosal processes. Squamosal ventral process anterior to quadratojugal dorsal process (0); squamosal ventral process overlapping the quadratojugal dorsal process (1) (Whatley 2005).
  27. Supratemporal. Present (1); absent (1) (Benton 1984a, 1985, 1988, 1990; Evans 1988; Dilkes 1998; Langer & Schultz 2000a; Whatley 2005; Hone & Benton 2008).
  28. Ventral margin of opisthotic paroccipital process. Convex (0); straight (1).
  29. Pterygoid midline suture length. Greater than or equal to the distance between the posterior margin of the suture and the basiptyergoid articulation (0); less than the distance between the posterior margin of the suture and the basiptyergoid articulation (1) (Whatley 2005).
  30. Elements forming the border of the suborbital fenestra. Ectopterygoid, palatine and maxilla (0); ectopterygoid and palatine only (1) (Dilkes 1995, 1998; Whatley 2005; Hone & Benton 2008).
  31. Occipital condyle position. Anterior to cranio-mandibular articulation (0); aligned to cranio-mandibular articulation (1) (Benton 1984a, 1985, 1988; Dilkes 1998; Langer & Schultz 2000a; Whatley 2005; Hone & Benton 2008).
  32. Basisphenoid and basisphenoid/parasphenoid lengths. Basisphenoid/parasphenoid longer (0); basisphenoid longer (1) (Langer & Schultz 2000a; Whatley 2005; Hone & Benton 2008).
  33. Relative positions of the basiptyergoid process of the basisphenoid and the ectopterygoid process of the pterygoid. At the same level (0), basiptyergoid process of the basisphenoid posterior to ectopterygoid process of the pterygoid (1) (Dilkes 1995).
  34. Basiptyergoid process dimensions (dorso-ventral length, antero-posterior width). Longer than wide (0); wider than long (1) (Langer & Schultz 2000a; Whatley 2005; Hone & Benton 2008).
  35. Mandible depth. Less than 0.25 of the total length (0); greater than 0.25 of the total length (1) (Benton 1984a, 1985, 1988, 1990; Dilkes 1995, 1998; Langer & Schultz 2000a; Whatley 2005; Hone & Benton 2008).
  36. Dentary length. Half, or less, than the total mandibular length (0); greater than half of the total mandibular length (1) (Benton 1990; Dilkes 1995; Langer & Schultz 2000a; Whatley 2005; Hone & Benton 2008).
  37. Medial maxillary groove. Absent (0); present but not reaching the anterior half of the maxilla (1); present and reaching the anterior half of the maxilla (2) (Benton 1984a, 1985, 1988, 1990; Dilkes 1995, 1998; Langer & Schultz 2000a; Langer *et al.* 2000a; Whatley 2005; Hone & Benton 2008).
  38. Maxillary area lateral to main groove. Narrower than the medial area (0); same width or broader than the medial area (1) (Benton 1990; Langer & Schultz 2000a; Langer *et al.* 2000a; Whatley 2005; Hone & Benton 2008).
  39. Maxillary cross-section lateral to main groove. Crest-shaped (0); cushion-shaped (1) (Langer *et al.* 2000a).
  40. Tooth-rows lateral to main maxillary groove. A single clear row (0); more than one clear row (1) (Langer & Schultz 2000a; Langer *et al.* 2000a).
  41. Number of tooth rows medial to main maxillary groove. Two rows and scattered teeth (0); three or more tooth rows (1) (Langer *et al.* 2000a).
  42. Occlusal tooth-rows on the anterior half of the maxilla. Four or more tooth-rows (0); less than four tooth rows (1) (Whatley 2005).
  43. Maxillary lingual teeth. Absent (0); scattered teeth (1); large number of teeth on the medial surface of the bone (2) (Benton 1984a, 1985, 1988, 1990; Dilkes 1995, 1998; Langer & Schultz 2000a; Langer *et al.* 2000a; Whatley 2005; Hone & Benton 2008).
  44. Maxillary teeth. Only conicals (0); conicals and 'pyramidal' (1) (Whatley 2005).
  45. Dentary teeth. Only conicals (0); conical and antero-posteriorly compressed (1) (Whatley 2005).
  46. Posterior-most dentary teeth. On the anterior half of dentary (0); on the posterior half of dentary (1) (Langer & Schultz 2000a; Hone & Benton 2008).
  47. Lingual dentary teeth. Absent (0); present and forming one row (1); present and forming more than one row (2) (Benton 1984a, 1985, 1990; Langer & Schultz 2000a; Langer *et al.* 2000a; Hone & Benton 2008).
  48. Dentary teeth on the dentary lingual surface. Scattered (0); crowded (1) (Benton 1985; Langer & Schultz 2000a; Langer *et al.* 2000a; Whatley 2005).
  49. Truncal vertebrae with ossified intercentrum. Present (0); absent (1) (Evans 1988; Dilkes 1995, 1998; Langer & Schultz 2000a; Whatley 2005; Hone & Benton 2008).
  50. Epiphyses on cervical postzygapophyses. Spine-shaped (0); crest-shaped (1) (Whatley 2005).
  51. Second sacral vertebra. With a notch between the iliac articular surface and the posterior process (0); posterior process continuous to the iliac articular surface (1) (Dilkes 1998; Whatley 2005).
  52. Caudal vertebrae neural spines. Height twice the length (0); height less than twice the length (1) (Dilkes 1998).
  53. Interclavicle. Posterior process longer than twice the lateral processes (0); posterior process shorter than twice the lateral process (1) (Dilkes 1998; Whatley 2005; Hone & Benton 2008).
  54. Posterior process of the coracoid. Present (0); absent (1) (Benton 1984a, 1985, 1988, 1990; Dilkes 1995, 1998; Langer & Schultz 2000a; Whatley 2005; Hone & Benton 2008).
  55. Dorsal margin of the ilium. Anterior process shorter than 15% of the posterior process (0); anterior process longer than 15% of the posterior process (1) (Dilkes 1995, 1998; Langer & Schultz 2000a; Whatley 2005; Hone & Benton 2008).
  56. Pubic tubercle. Present (0); absent (1) (Whatley 2005).
  57. Internal trochanter. Continuous to the femoral head (0); separated from femoral head (1) (Whatley 2005).
  58. Relative size of astragalar articular facets. Tibial facet greater than centrale facet (0); centrale facet greater than tibial facet (1) (Langer & Schultz 2000a; Langer *et al.* 2000a; Hone & Benton 2008).
  59. Metatarsal I. Longer than broad (0); broader than long (1) (Hone & Benton 2008).

### Synapomorphy list

**Node 1: (Rhynchosauridae):** character 47 (0→2).

**Node 2:** characters 5, 12, 52, 55, 59.

**Node 3:** characters 24, 43 (1→2).

**Node 4:** characters 6, 49.

**Node 5: (Hyperodapedontinae):** characters 1, 3, 7, 9, 11, 13, 31.

**Node 6:** characters 20, 34, 40, 50.

### 5.3. Appendix 3. Character state matrix

Missing data are marked as "?", non applicable characters as "-" and variable condition under "{ }".

```

Mesosuchus
000000-0-1 0000001000 0000000100 000000---- --00000000 000000000
Howesia
00000?-0-1 0001001000 0000??0010 0000??---- -010000?0? 00??01000
Rhynchosaurus
0000000001 0000010000 00000000?0 0000010000 01100?20?? 00000??00
Stenaulorhynchus
000110000? 0101110010 0101000011 0000002000 1120002100 010011001
'Rincossauro de Mariante'
0100100000 0101111100 1011000100 0100??2000 11200?21?? ??????????
Foðonyx
000111000? 0100101000 1110??0111 0010?????0? ??1????201? ??????????1
Isalorhynchus
111?111111 1010?????00 ??1?11?001 1100110110 0101111010 11111111?
T. sulcognathus
1111111110 1110011111 1110111001 1101112001 1011112111 ??????1?1?
Hyperodapedon
111011101{0 1} 1{0 1}11011011 {0 1}110111{0 1}{0 1}1 11{0 1}111{0 1}{0 1}11 10{0 1}111{0 1}
2}011 111110{0 1}11

```

## 6. References

- Andreis, R. R., Bossi, G. E. & Montardo, D. K. 1980. O Grupo Rosário do Sul (Triássico) no Rio Grande do Sul. In Landim, P. M. B. (ed) *XXXI Congresso Brasileiro de Geologia*, 659–73. Camboriú: Sociedade Brasileira de Geologia.
- Azevedo, S. A. 1982. *Scaphonyx sulcognathus* (sp. nov.) um novo rincossaurídeo do Neotriássico do Rio Grande do Sul, Brasil. Unpublished Thesis, Instituto de Geociências, Universidade Federal do Rio Grande do Sul, Porto Alegre. 86 pp.
- Azevedo, S. A. 1984. Sobre a presença de *Scaphonyx sanjuanensis* Sill, 1970 no Neotriássico do Rio Grande do Sul, Brasil. *Pesquisas* **16**, 69–75.
- Azevedo, S. A. 1987. Estudo paleoecológico de *Scaphonyx sulcognathus*. In Moura, J. A., Gilson, H. M. N., Campos, D. A., Beurlen, G., Macedo, A. C. M. & Brito, I. A. M. (eds) *X Congresso Brasileiro de Paleontologia*, 115–21. Rio de Janeiro: Sociedade Brasileira de Paleontologia.
- Azevedo, S. A., Fariña, R. A. & Schultz, C. L. 1989. The relationships between morpho-functional changes and variation in alimentary habit among rhynchosaurs of the South American Triassic. *Annales de la Société Royale Zoologique de Belgique* **119**, 11.
- Azevedo, S. A., Schultz, C. L. & Barberena, M. C. 1990. Novas evidências bioestratigráficas e paleoecológicas na análise da evolução explosiva dos rincossauros do Triássico. *Paula-Coutiana* **4**, 23–33.
- Azevedo, S. A. & Schultz, C. L. 1987. *Scaphonyx sulcognathus* (sp. nov.), um novo rincossaurídeo do neotriássico do Rio Grande do Sul, Brasil. In Moura, J. A., Gilson, H. M. N., Campos, D. A., Beurlen, G., Macedo, A. C. M. & Brito, I. A. M. (eds) *X Congresso Brasileiro de Paleontologia*, 99–113. Rio de Janeiro: Sociedade Brasileira de Paleontologia.
- Barberena, M. C., Gomes, Araujo, D. F., Lavina, E. L. & Azevedo, S. A. K. 1985. O estado atual do conhecimento sobre os tetrápodos Permianos e Triássicos do Brasil Meridional. *Coletâneas de trabalhos paleontológicos. Série Geológica* **27**, 21–28.
- Barros, R. C. R. 2004. *Os rincossauros do Rio Grande do Sul*. Unpublished Thesis, Instituto de Geociências, Universidade Federal do Rio Grande do Sul, Porto Alegre. 91 pp.
- Benton, M. J. 1983. The Triassic reptile *Hyperodapedon* from Elgin: functional morphology and relationships. *Philosophical Transactions of the Royal Society of London, Series B* **302**, 605–717.
- Benton, M. J. 1984a. The relationships and early evolution of the Diapsida. *Symposia of the Zoological Society of London* **52**, 575–96.
- Benton, M. J. 1984b. Tooth form, growth, and function in Triassic rhynchosaurs (Reptilia, Diapsida). *Palaeontology* **27**, 373–776.
- Benton, M. J. 1985. Classification and phylogeny of the diapsid reptiles. *Zoological Journal of the Linnean Society* **84**, 97–154.
- Benton, M. J. 1988. The phylogeny of rhynchosaurs (Reptilia, Diapsida), and two new species. In Currie, P. M. & Coster, E. H. (eds) *Fourth Symposium on Mesozoic Terrestrial Ecosystems, Short Papers. Occasional Papers of the Tyrrell Museum of Palaeontology* **3**, 2–17. Drumheller, Alberta: Royal Tyrrell Museum of Palaeontology.
- Benton, M. J. 1990. The species of *Rhynchosaurus*, a rhynchosaur (Reptilia, Diapsida) from the Middle Triassic of England. *Philosophical Transactions of the Royal Society of London, Series B* **328**, 213–306.
- Benton, M. J. 1993. Reptilia. In Benton, M. J. (ed.) *The Fossil Record* **2**, 681–715. London: Chapman & Hall.
- Broom, R. 1906. On the South African Diaptosaurian reptile *Howesia*. *Proceedings of the Royal Society of London* **1906**, 591–600.
- Buffetaut, E. 1983. *Isalorhynchus genovefae*, n. g. n. sp. (Reptilia, Rhyncocephalia), um nouveau Rhyncoceure du Trias de Madagascar. *Neues Jahrbuch für Geologie und Paläontologie, Monatshefte* **1983**, 465–80.
- Chatterjee, S. 1969. Rhynchosaurs in time and space. *Proceedings of the Geological Society, London* **1958**, 203–08.
- Chatterjee, S. 1974. A rhynchosaur from the Upper Triassic Maleri Formation of India. *Philosophical Transactions of the Royal Society of London, Series B* **267**, 209–61.
- Chatterjee, S. 1980. The evolution of rhynchosaurs. *Mémoires de la Société Géologique de France*, ns **139**, 57–65.
- Contreras, V. H. & Bracco, A. 1989. *Scaphonyx sulcognathus* Azevedo & Schultz, 1987, especie tipo de un nuevo genero de la subfamilia Paradapedontinae (Reptilia: Rhynchosauridae). In Contreras, V. H. (ed.) *Jornadas Argentinas de Paleontología de Vertebrados*, 11–12. San Juan: Asociación Paleontológica Argentina.
- Currie, B. S., Colombi, C. E., Tabor, N. J., Shipman, T. C. & Montañez, I. P. 2008. Stratigraphy and architecture of the Upper Triassic Ischigualasto Formation, Ischigualasto Provincial Park, San Juan, Argentina. *Journal of South American Earth Sciences* **27**, 74–87.
- Desojo, J. B. & Báez, A. M. 2007. Cranial morphology of the Late Triassic South American archosaur *Neoaetosauroides engaeus*: evidence for aetosaurian diversity. *Palaeontology* **50**, 267–76.
- Dilkes, D. W. 1995. The rhynchosaur *Howesia browni* from the Lower Triassic of South Africa. *Palaeontology* **38**, 665–85.
- Dilkes, D. W. 1998. The Early Triassic rhynchosaur *Mesosuchus browni* and the interrelationships of basal archosauromorph reptiles. *Philosophical Transactions of the Royal Society of London, Series B* **353**, 501–41.
- Evans, S. E. 1988. The early history and relationships of the Diapsida. In Benton, M. J. (ed.) *The Phylogeny and Classification of the Tetrapods*, 221–60. Oxford: Clarendon Press.
- Fariña, R. A. 1991. Anatomia funcional mastigatória em *Scaphonyx sulcognathus*. Unpublished Thesis, Instituto de Geociências, Universidade Federal do Rio Grande do Sul, Porto Alegre. 41 pp.
- Furin, S., Preto, N., Rigo, M., Roghi, G., Gianolla, P., Crowley, J. L. & Bowring, S. A. 2006. High-precision U–Pb zircon age from the Triassic of Italy: implications for the Triassic time scale and the Carnian origin of calcareous nannoplankton and dinosaurs. *Geology* **34**, 1009–12.
- Gallet, Y., Krystyn, L., Besse, J. & Marcoux, J. 2003. Improving the Upper Triassic numerical time scale from cross-correlation

- between Tethyan marine sections and the continental Newark Basin sequence. *Earth and Planetary Science Letters* **212**, 255–61.
- Gervais, P. 1859. *Zoologie et Paléontologie Française*, 2nd edn. Paris: Arthus Bertrand. 544 pp.
- Goloboff, P., Farris, J. S. & Nixon, K. C. 2008. TNT, a free program for phylogenetic analyses. *Cladistics* **24**, 774–86.
- Gower, D. J. & Nesbitt, S. 2006. The braincase of *Arizonasaurus babbitti* – further evidence for the non-monophyly of ‘rauisuchian’ archosaurs. *Journal of Vertebrate Paleontology* **26**, 79–87.
- Gower, D. J. & Sennikov, A. G. 1996. Morphology and phylogenetic informativeness of early archosaur braincases. *Palaeontology* **39**, 883–906.
- Haughton, S. H. 1932. On a collection of Karoo vertebrates from Tanganyika territory. *Quarterly Journal of the Geological Society, London* **88**, 643–62.
- Hone, D. W. E. & Benton, M. J. 2008. A new genus of rhynchosaur from the Mid Triassic of SW England. *Palaeontology* **51**, 95–115.
- Huene, F. von 1926. Gondwana-Reptilien in Südamerika. *Palaeontologia Hungarica* **II**, 1–102.
- Huene, F. von 1929. Über Rhynchosaurier und andere Reptilien aus den Gondwana-Ablagerungen Südamerikas. *Geologische und Palaeontologische Abhandlungen* **17**, 1–61.
- Huene, F. von 1938. *Stenaulorhynchus*, ein Rhynchosauride der ostafrikanischen Obertrias. *Nova Acta Leopoldina N.F.* **6**, 83–121.
- Huene, F. von 1939. Die Verwandtschaftsgeschichte der Rhynchosauriden des südamerikanischen Gondwanalandes. *Physis* **14**, 499–523.
- Huene, F. von 1942. *Die fossilen Reptilien des südamerikanischen Gondwanalandes*. Munich: C. H. Beck. 342 pp.
- Huxley, T. H. 1859. *Postscript*: Murchinson, R. I. On the sandstones of Morayshire (Elgin & c.) containing reptilian remains, and their relations to the Old Red Sandstone of that Country. *Quarterly Journal of the Geological Society, London* **15**, 435–36.
- Huxley, T. H. 1887. Further observations upon *Hyperodapedon gordoni*. *Quarterly Journal of the Geological Society, London* **25**, 138–52.
- Kent, D. V., Muttoni, G. & Brack, P. 2006. Reply to ‘Discussion of “Magnetostatigraphic confirmation of a much faster tempo for sea-level change for the Middle Triassic Latemar platform carbonates” by D. V. Kent, G. Muttoni & P. Brack [Earth and Planetary Science Letters **228** (2004), 369–77]’ by L. Hinnov. *Earth and Planetary Science Letters* **243**, 847–50.
- Langer, M. C. 1996. *Rincossauros sul-brasileiros: histórico e filogenia*. Unpublished Thesis, Instituto de Geociências, Universidade Federal do Rio Grande do Sul, Porto Alegre. 361 pp.
- Langer, M. C. 2005. Studies on continental Late Triassic tetrapod biochronology. I. The type locality of *Saturnalia tupiniquim* and the faunal succession in south Brazil. *Journal of South American Earth Sciences* **19**, 205–18.
- Langer, M. C., Boniface, M., Cuny, G. & Barbieri, L. 2000a. The phylogenetic position of *Isalorhynchus genovefae*, a Late Triassic rhynchosaur from Madagascar. *Annales de Paléontologie* **86**, 101–27.
- Langer, M. C., Ferigolo, J. & Schultz, C. L. 2000b. Heterochrony and tooth evolution in hyperodapedontine rhynchosaurs (Reptilia, Diapsida). *Lethaia* **33**, 119–28.
- Langer, M. C., Ribeiro, A. M., Schultz, C. L. & Ferigolo, J. 2007. The continental tetrapod-bearing Triassic of South Brazil. In Lucas, S. G. & Spielmann, J. A. (eds) *The Global Triassic: New Mexico Museum of Natural History and Science Bulletin*, 201–218. Albuquerque, New Mexico: New Mexico Museum of Natural History and Science.
- Langer, M. C. & Schultz, C. L. 2000a. A new species of the Late Triassic rhynchosaur *Hyperodapedon* from the Santa Maria Formation of south Brazil. *Palaeontology* **43**, 633–52.
- Langer, M. C. & Schultz, C. L. 2000b. Rincossauros – herbívoros cosmopolitas do Triássico. In Holz, M. & de Ros, L. F. (eds) *Palaeontologia do Rio Grande do Sul*, 246–72. Porto Alegre: CIGO/UFRGS.
- Lydekker, R. 1885. Reptilia and Amphibia of the Maleri and Denwa groups. *Palaeontologia Indica* **4**, 1–28.
- Lydekker, R. 1888. *Catalogue of the fossil Reptilia and Amphibia in the British Museum (Natural History)*, 296–301. London: British Museum.
- Matthews, S. C. 1973. Notes on open nomenclature and on synonymy lists. *Palaeontology* **16**, 713–19.
- Montefeltro, F. C. 2008. *Inter-relações filogenéticas dos rincossauros (Diapsida, Archosauromorpha)*. Unpublished Thesis, Biology Department, Universidade de São Paulo, Ribeirão Preto. 203 pp.
- Montefeltro, F. C. & Langer, M. C. 2008. Inter-relações filogenéticas dos rincossauros (Diapsida, Archosauromorpha). In Langer, M. C., Bittencourt, J. S. & Castro, M. C. (eds) *VI Simpósio Brasileiro de Paleontologia de Vertebrados*, 133–5. Ribeirão Preto: Sociedade Brasileira de Paleontologia.
- Muttoni, G., Kent, D. V., Di Stefano, P., Gullo, M., Nicora, A., Tait, J. & Lowrie, W. 2001. Magnetostratigraphy and biostratigraphy of the Carnian/Norian boundary interval from the Pizzo Mondello section (Sicani Mountains, Sicily). *Palaeogeography, Palaeoclimatology, Palaeoecology* **166**, 383–99.
- Muttoni, G., Kent, D. V., Olsen, P. E., Di Stefano, P., Lowrie, W., Bernasconi, S. M. & Hernández, F. M. 2004. Tethyan magnetostratigraphy from Pizzo Mondello (Sicily) and correlation to the Late Triassic Newark astrochronological polarity time scale. *Geological Society of America Bulletin* **116**, 1043–58.
- Nesbitt, S. & Whatley, R. 2004. The first discovery of a rhynchosaur from the Upper Moenkopi Formation (Middle Triassic) of northern Arizona. *PaleoBios* **24**, 1–10.
- Ogg, J. G. 2004. The Triassic period. In Gradstein, F. M., Ogg, J. G. & Smith, A. G. (eds) *A Geologic Time Scale 2004*, 271–306. Cambridge: Cambridge University Press.
- Osborn, H. F. 1903. The reptilian subclasses Diapsida and Synapsida and the early history of the Diaptosauria. *Memoirs of the American Museum of Natural History* **1**, 449–507.
- Owen, R. 1842. Description of an Extinct Lacertilian Reptile, *Rhynchosaurus articeps* Owen, of which the Bones and Foot-prints characterize the Upper New Red Sandstone at Grinshill, near Shrewsbury. *Transactions of the Cambridge Philosophical Society* **7**, 355–69.
- Romer, A. S. 1956. *Osteology of Reptiles*. Chicago: The University of Chicago Press. 772 pp.
- Romer, A. S. 1962. La evolución explosiva de los rhynchosaurios del Triásico. *Revista del Museo Argentino de Ciencias Naturales Bernardino Rivadavia e Instituto Nacional de Investigación de las Ciencias Naturales. Ciencias Zoológicas* **VIII**, 1–14.
- Rubidge, B. S. 2005. 27th Du Toit Memorial Lecture – Re-uniting lost continents – Fossil reptiles from ancient Karoo and their wanderlust. *South African Journal of Geology* **108**, 135–72.
- Schultz, C. L. 1986. *Osteologia parcial do pós crânio de Scaphonyx sulcognathus Azevedo 1982 (Reptilia, Diapsida, Rhynchocephalia)*. Instituto de Geociências, Universidade Federal do Rio Grande do Sul, Porto Alegre. 139 pp.
- Schultz, C. L. 1991. *Os rincossauros Sul-Americanos e suas relações com outros representantes do grupo*. Unpublished Thesis, Instituto de Geociências, Universidade Federal do Rio Grande do Sul, Porto Alegre. 416 pp.
- Schultz, C. L. 1995. Subdivisão do Triássico do RS com base em macrofósseis: problemas e perspectivas. *Comunicações do Museu de Ciências e Tecnologia* **1**, 25–32.
- Schultz, C. L. 1999. An example of paleopathology in rhynchosaur specimens of southern Brazilian Triassic. In Césari, S. & Damborenea, S. (eds) *XV Jornadas Argentinas de Paleontología de Vertebrados*, 24. La Plata & Luján: Asociación Paleontológica Argentina.
- Schultz, C. L. & Azevedo, S. A. 1990. Dados preliminares sobre a ocorrência de uma nova forma de rincossauro para o Triássico do Rio Grande do Sul- Brasil. *Paula-Coutiana* **4**, 35–44.
- Sill, W. D. 1970. *Schaphonyx sanjuanensis*, nuevo rincosaurio (Reptilia) de la Formación Ischigualasto, Triásico de San Juan, Argentina. *Ameghiniana* **7**, 341–54.
- Tupi-Caldas, J. A. L. (ed.) 1933. *Curso Geral de Mineralogia e Geologia, aplicada ao Brasil*. Porto Alegre: Edições da Livraria Globo. 349 pp.
- Walker, J. D. & Geissman, J. W. 2009. Compilers, 2009. Geologic Time Scale: Geological Society of America.
- Whatley, R. 2005. Phylogenetic relationship of *Isalorhynchus genovefae*, the rhynchosaur (Reptilia, Archosauromorpha) from Madagascar. Unpublished Thesis, University of California, Santa Barbara. 276 pp.
- Watson, D. M. S. 1912. *Mesosuchus browni*, gen. et spe. Nov. *Records of the Albany Museum* **2**, 298–99.
- Woodward, A. S. 1907. On some dinosaurian bones from the state of Rio Grande do Sul. *Revista do Museu Paulista* **7**, 137–50.
- Zerfass, H., Lavina, E. L., Schultz, C. L., Garcia, A. G. V. Faccini, U. F. & Chemale, F. Jr. 2003. Sequence stratigraphy of continental Triassic strata of southernmost Brazil, a contribution to Southwestern Gondwana palaeogeography and palaeoclimate. *Sedimentary Geology* **161**, 85–105.